Measuring Light-Meson Resonances in the $\omega\pi^-\pi^0$ and $K_S^0 K^-$ Final States at COMPASS

Julien Beckers* and Philipp Haas (Technical University of Munich)

for the COMPASS Collaboration

HADRON 2025 (Osaka, Japan)

March 27th, 2025

Excited Light Mesons at COMPASS

- Inelastic scattering reactions of high-energetic meson beam

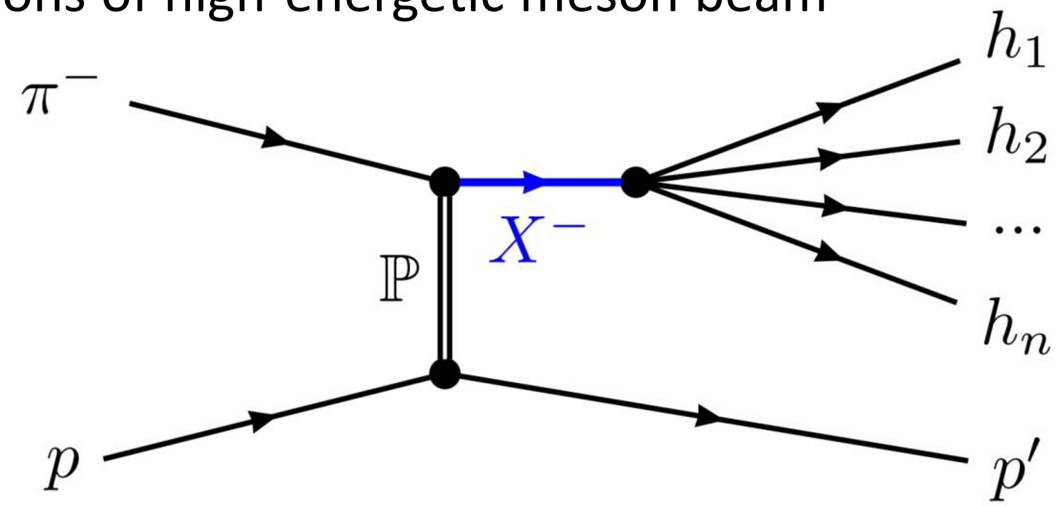

- Strong interaction (Pomeron exchange) between beam meson and target proton
- Intermediate hadronic resonances X^- are created, then decay into n-body final state

  → wide range of allowed (spin) quantum numbers

  → many different final states can be produced

- Final-state particles measured in the COMPASS spectrometer

Excited Light Mesons at COMPASS

- Inelastic scattering reactions of high-energetic meson beam

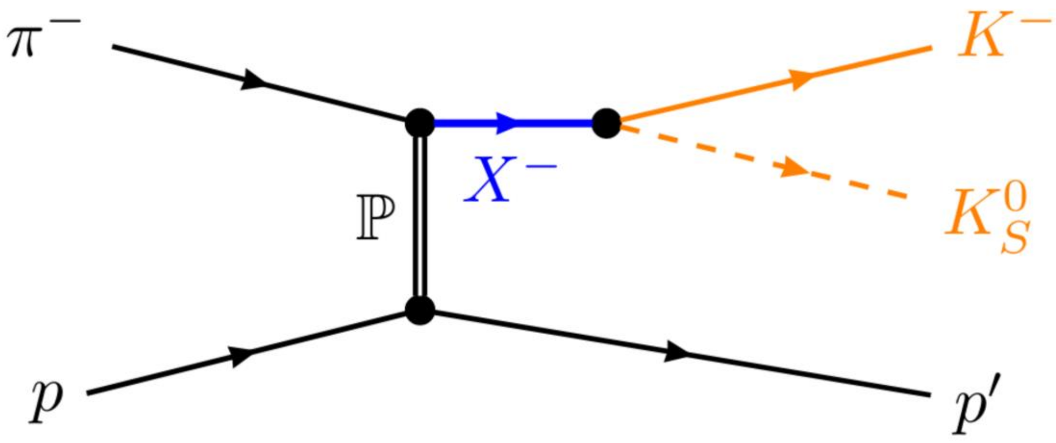

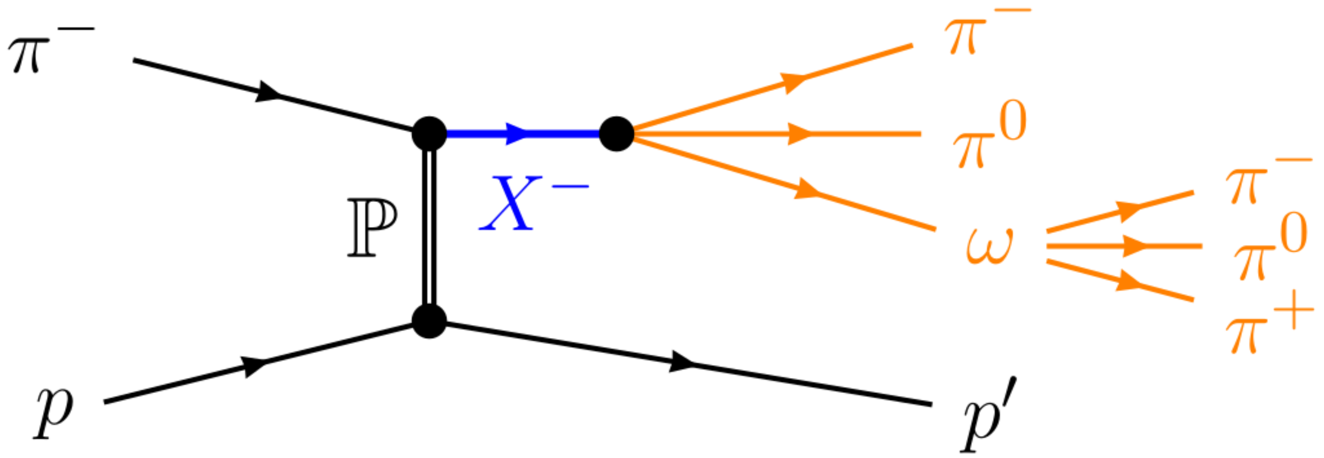

- Strong interaction (Pomeron exchange) between beam meson and target proton
- Intermediate hadronic resonances X^- are created, then decay into n-body final state

  → wide range of allowed (spin) quantum numbers

  → many different final states can be produced, here: $K_S^0 K^-$ and $\omega\pi^-\pi^0$
- Final-state particles measured in the COMPASS spectrometer

The COMPASS Experiment at CERN

Large-acceptance magnetic spectrometer @ CERN-SPS

Beam:

- Secondary hadrons (π^-, K^-) at $190\ \mathrm{GeV}/c$
- Cherenkov detectors identify beam particles

The COMPASS Experiment at CERN

Large-acceptance magnetic spectrometer @ CERN-SPS

Beam:

- Secondary hadrons (π^-, K^-) at $190\ \mathrm{GeV}/c$
- Cherenkov detectors identify beam particles

Spectrometer:

- Liquid-hydrogen target
- Two-stage spectrometer setup
- Cherenkov detector (RICH1) identifies final-state particles in momentum range $3\ \mathrm{GeV}/c\ - 60\ \mathrm{GeV}/c$

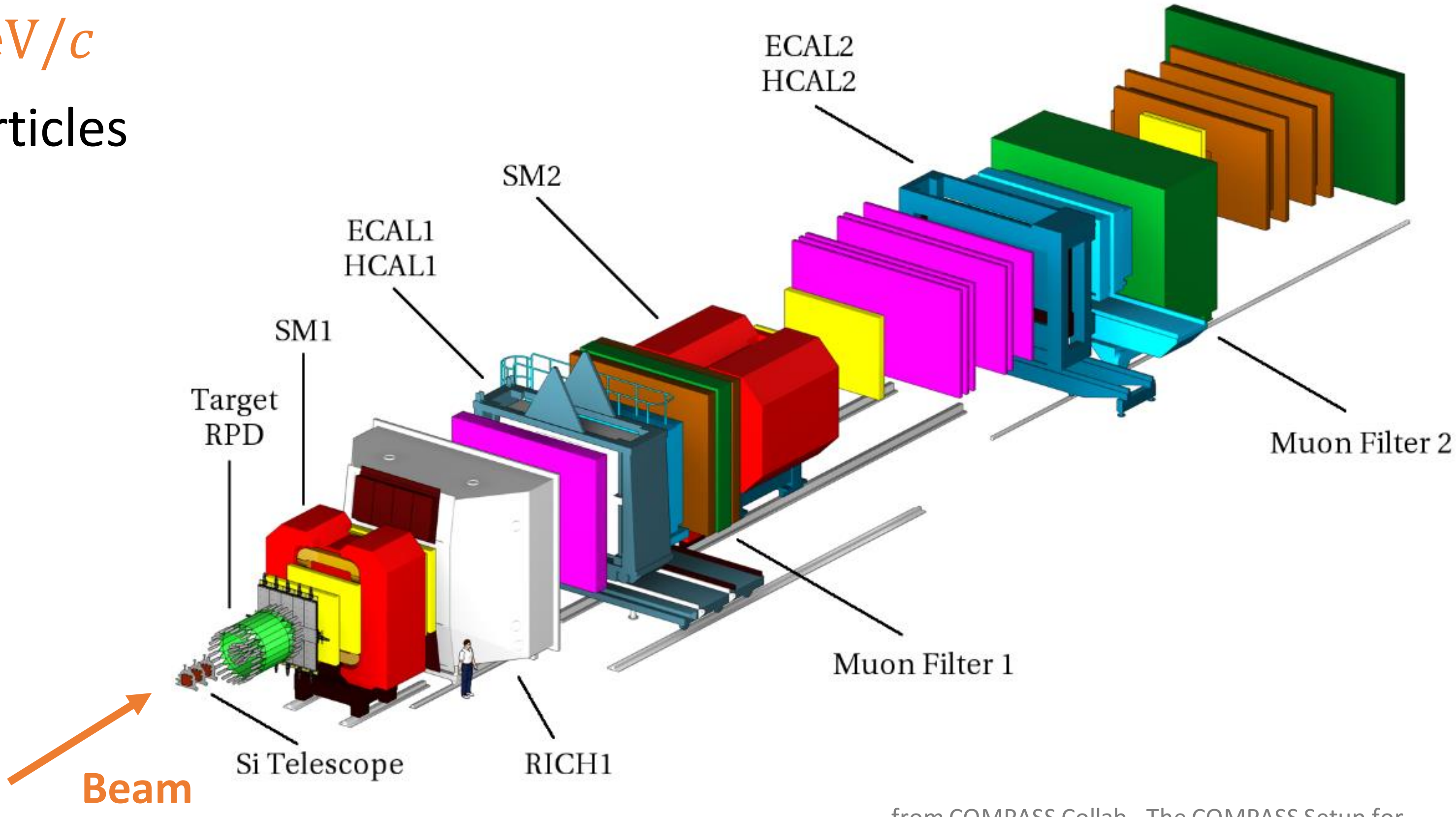

from COMPASS Collab., The COMPASS Setup for Physics with Hadron Beams (Nucl. Instrum. Methods Phys. Res. A 779 (2014), pp. 69–115)

Measuring Light-Meson States

Goal: Identify produced X^- resonances

- Measure their quantum numbers
- Measure their masses and widths

$\rightarrow$ **Partial-wave analysis** in two stages

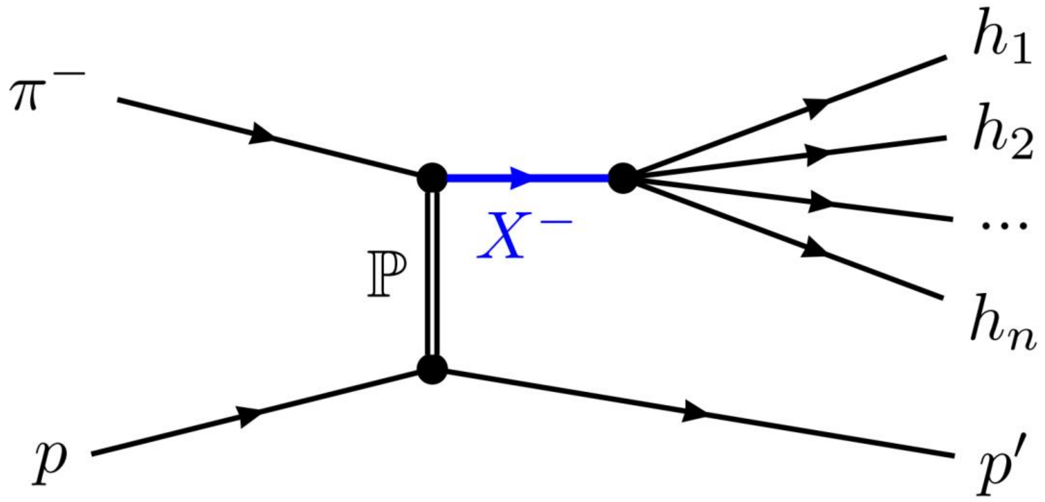

Partial-Wave Analysis Procedure

First stage: **Partial-Wave Decomposition**

$$\frac{dN}{d\Phi(\tau)dm_X dt'} \sim \quad I(m_X, t'; \tau) = \left| \sum_a T_a(m_X, t')\, \psi_a(m_X, \tau) \right|^2$$

- Decompose total process amplitude into **partial waves**
  - Depend on quantum numbers and decay $a = J^{PC} M$ <decay>

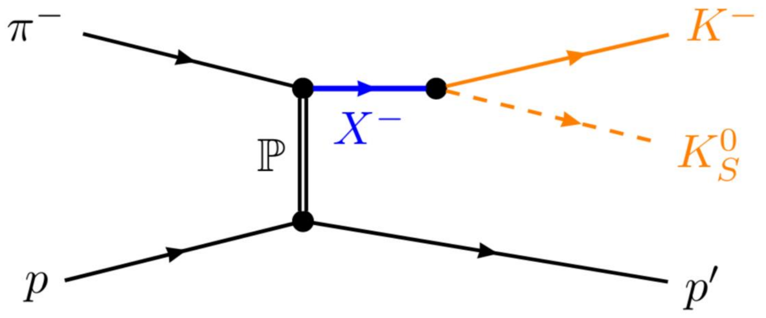

Partial-Wave Analysis Procedure

First stage: **Partial-Wave Decomposition**

$$\frac{dN}{d\Phi(\tau)dm_X dt'} \sim \quad I(m_X, t'; \tau) = \left| \sum_a T_a(m_X, t')\, \psi_a(m_X, \tau) \right|^2$$

- Decompose total process amplitude into **partial waves**

- Amplitudes split into
  - **production and propagation** of X^-: $T_a(m_X, t')$

  and
  - **decay** of X^-: $\psi_a(\tau)$

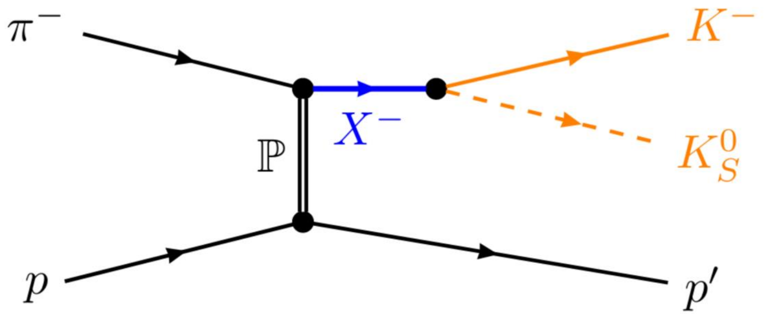

Partial-Wave Analysis Procedure

First stage: **Partial-Wave Decomposition**

$$\frac{dN}{d\Phi(\tau)dm_X dt'} \sim \quad I(m_X, t'; \tau) = \left|\sum_a T_a(m_X, t')\, \psi_a(m_X, \tau)\right|^2$$

- Decompose total process amplitude into **partial waves**

- Amplitudes split into production/propagation and decay of X^-

- Dependence of T_a on (m_X, t') unknown

→ fit $I(m_X, t'; \tau)$ to data **independently in (m_X, t') cells**

→ extract constant $\{T_a\}$ in each cell

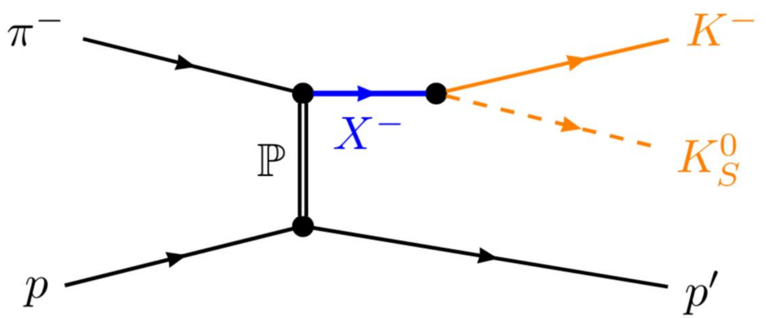

Partial-Wave Analysis Procedure

Second stage: **Resonance-Model Fit**

Goal: Extract **mass and width of X^-** from partial-wave decomposition

Build model for m_X-dependence of the partial-wave amplitudes

Coherent sum of:

- Set of **resonances** contributing to the process
- **Background processes** to be parametrized

→ χ^2 fit to the partial-wave distributions

→ partial-wave intensities and all relative phases

→ Obtain parameters of included resonances

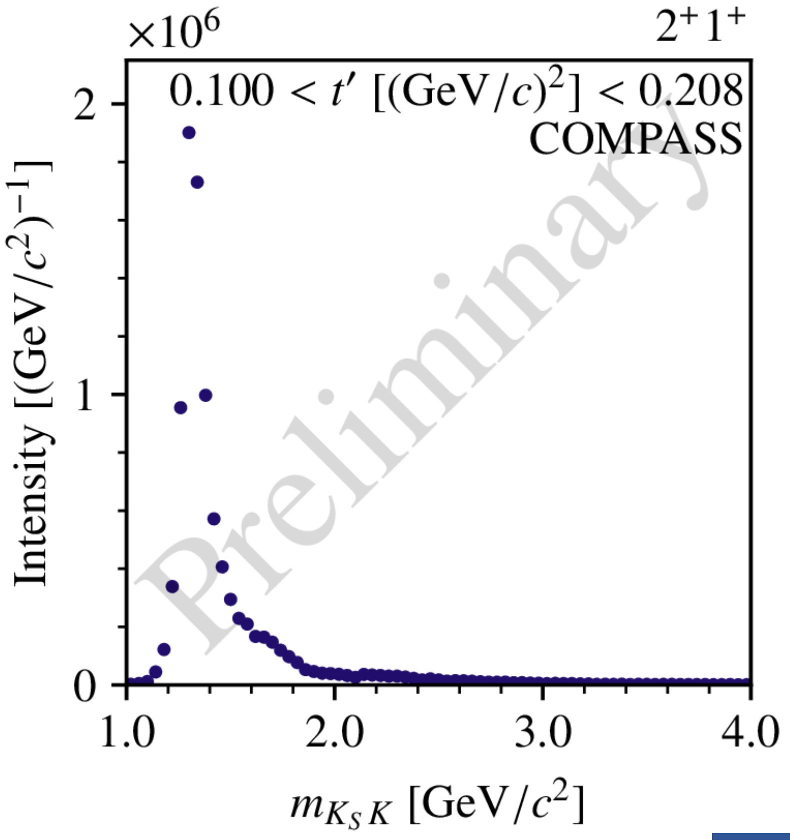

Partial-Wave Analysis Procedure

Second stage: **Resonance-Model Fit**

Goal: Extract **mass and width of X^-** from partial-wave decomposition

Build model for m_X-dependence of the partial-wave amplitudes

Coherent sum of:

- Set of **resonances** contributing to the process
- **Background processes** to be parametrized

→ χ^2 fit to the partial-wave distributions

→ partial-wave intensities and all relative phases

→ Obtain parameters of included resonances

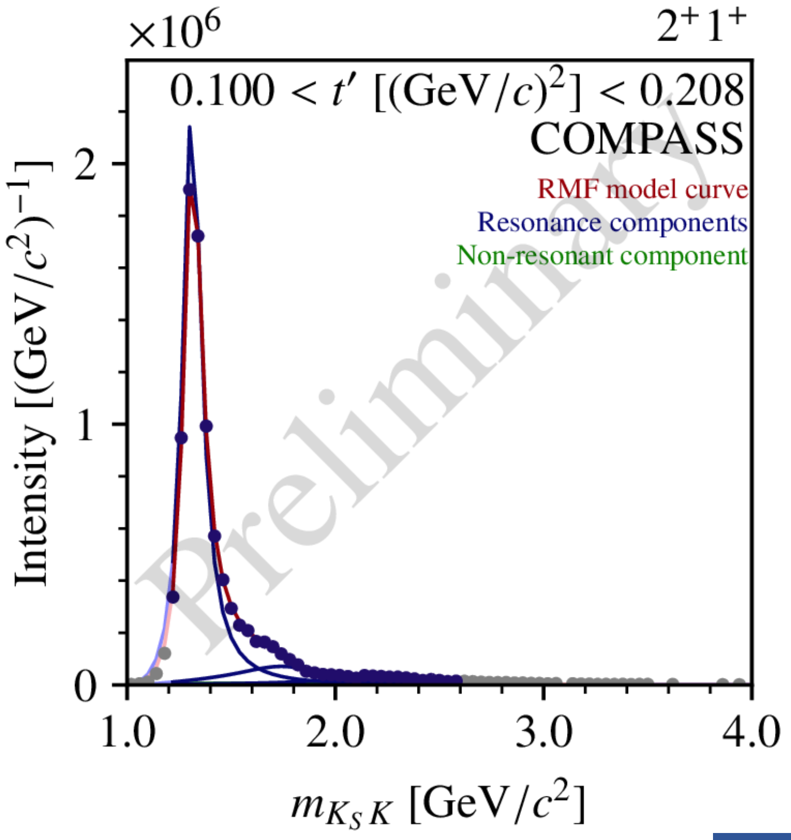

The $K_S^0 K^-$ Final State

First analysis of the COMPASS $K_S^0 K^-$ data

Accessible states: $\boldsymbol{a_J}$ **for even** $\boldsymbol{J}$ $(2^{++}, 4^{++}, \dots)$

- Overlapping quantum numbers with $\pi^-\pi^-\pi^+$, but
- higher invariant masses due to 2 kaons, and
- only even spins J dominant at COMPASS

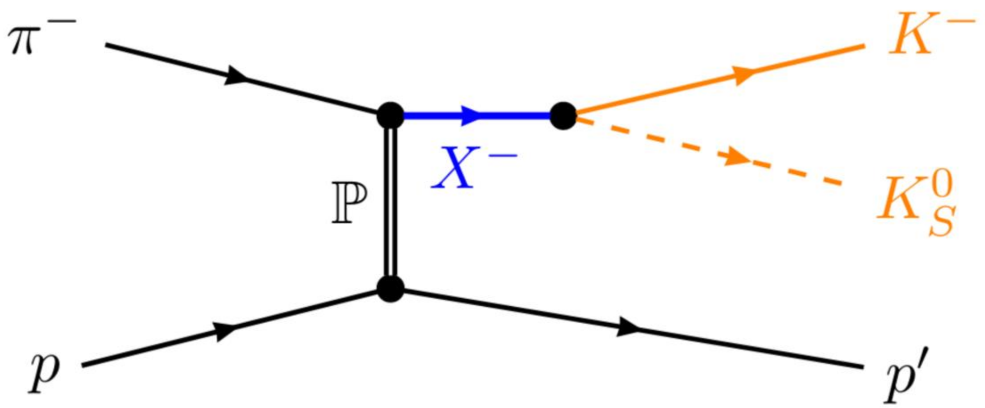

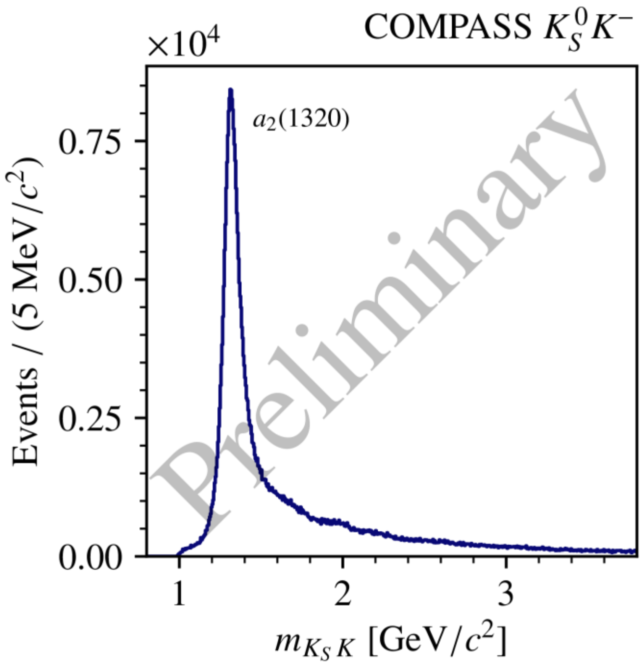

Challenges:

- Ambiguities in the partial-wave decomposition
- Less interference information between waves

The $J^{PC} = 2^{++}$ Sector in $K_S^0 K^-$

$a_2(1320)$:

- Very prominent signal

$$m_0 = 1316.63 \pm 0.2\, ^{+2.23}_{-2.33}\ \mathrm{MeV}/c^2$$
$$\Gamma_0 = 109.5 \pm 0.4\, ^{+2.6}_{-2.0}\ \mathrm{MeV}/c^2$$

$a_2(1700)$:

- Necessary to describe high-mass shoulder
- Larger width than previous measurements

$$m_0 = 1748 \pm 4\, ^{+13}_{-86}\ \mathrm{MeV}/c^2$$
$$\Gamma_0 = 534 \pm 9\, ^{+26}_{-230}\ \mathrm{MeV}/c^2$$

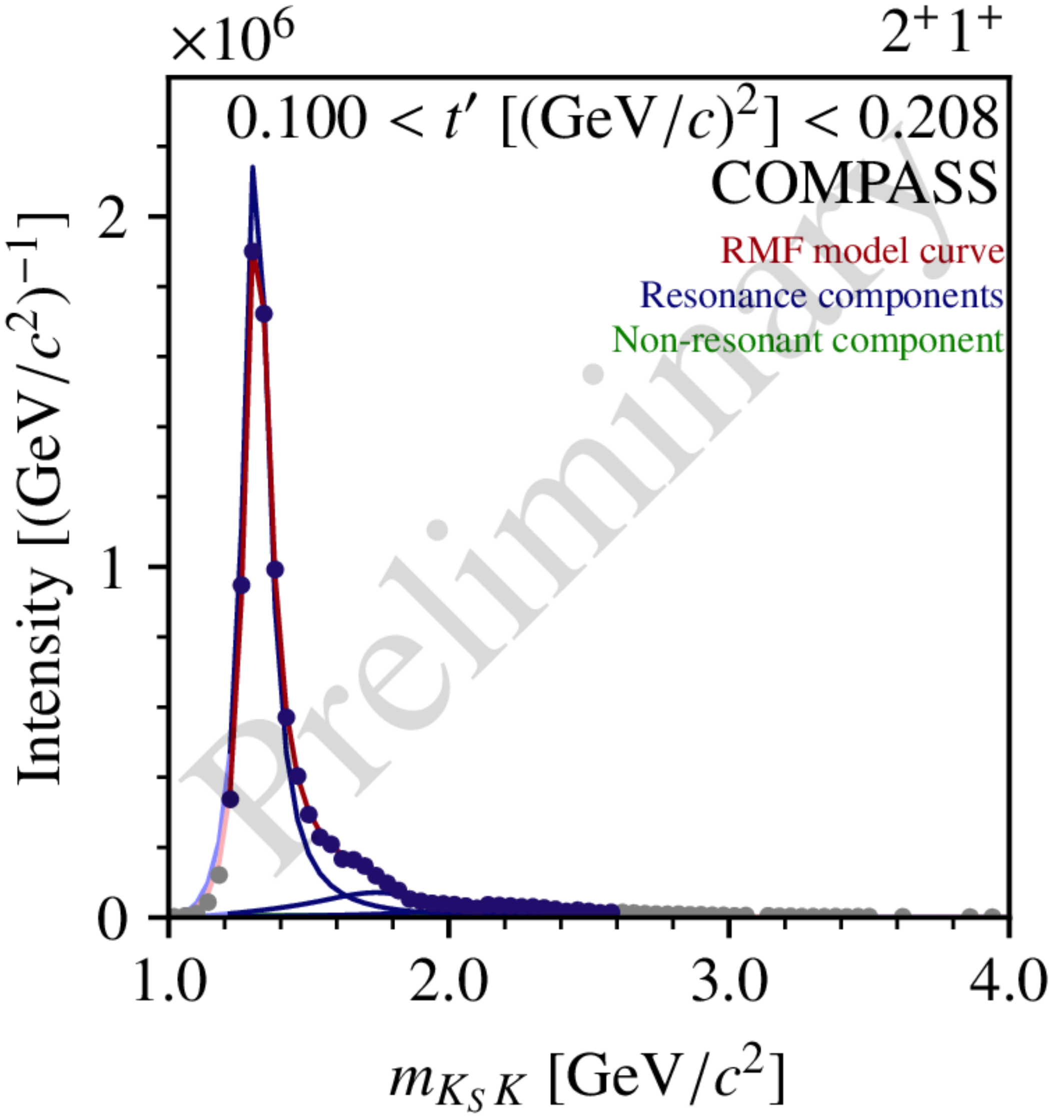

The $J^{PC} = 2^{++}$ Sector in $K_S^0 K^-$

a_2'':

- Indications of a higher-mass state above 2 GeV/c^2

$$m_0 = 2124 \pm 5\ ^{+37}_{-9}\,\mathrm{MeV}/c^2$$
$$\Gamma_0 = 527 \pm 13\ ^{+55}_{-250}\ \mathrm{MeV}/c^2$$

- Several states claimed by previous experiments, scattered in this invariant mass range

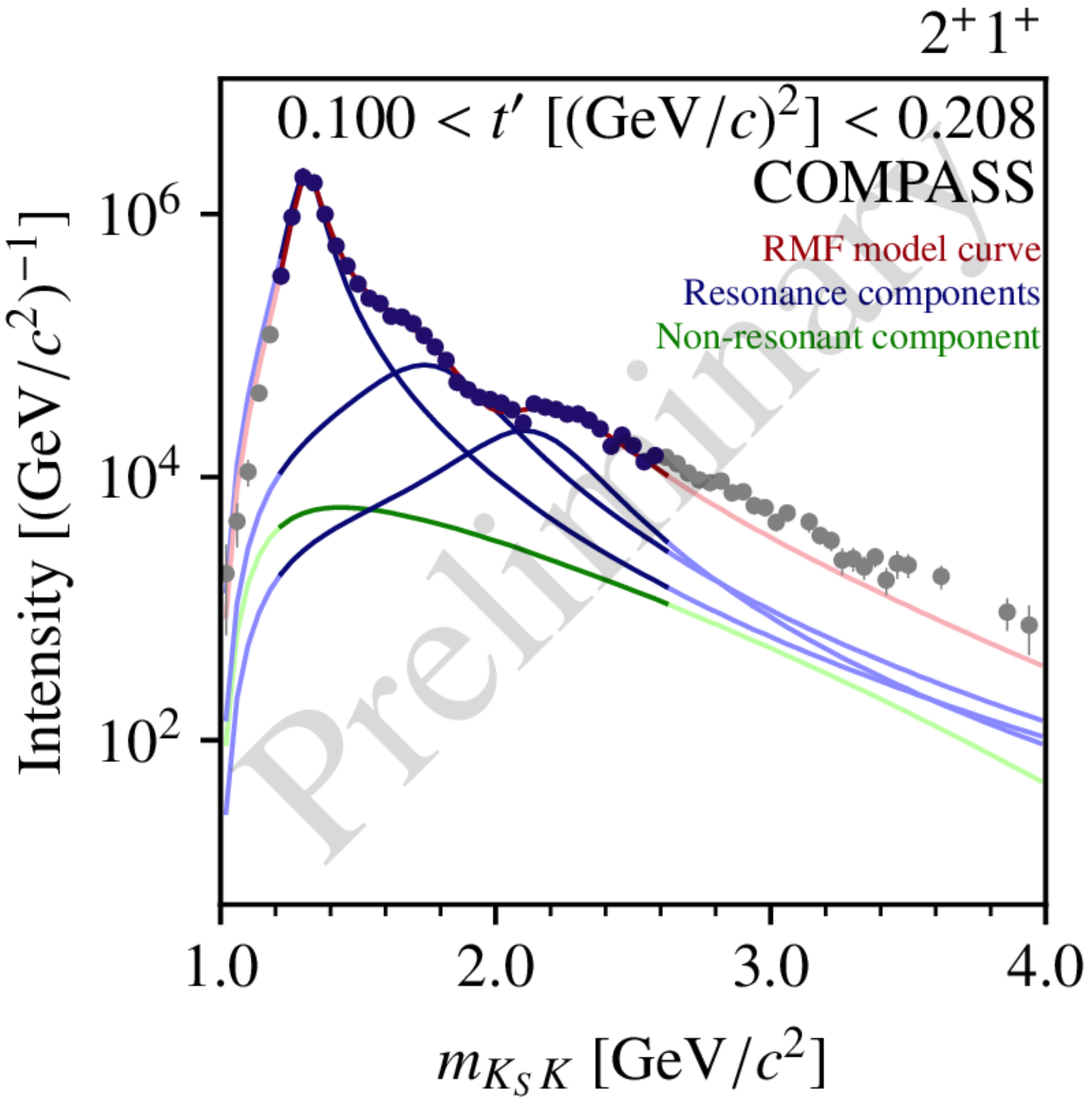

cf Particle Data Group, Phys. Rev. D **110**, 030001 (2024)

The $J^{PC} = 4^{++}$ Sector in $K_S^0 K^-$

$a_4(1970)$:

- Precise measurement of the well-known state
- Clear peak and phase movement well-described

$$m_0 = 1952.2 \pm 1.8\,^{+3.0}_{-3.5}\ \mathrm{MeV}/c^2$$
$$\Gamma_0 = 327 \pm 4\,^{+6}_{-6}\ \mathrm{MeV}/c^2$$

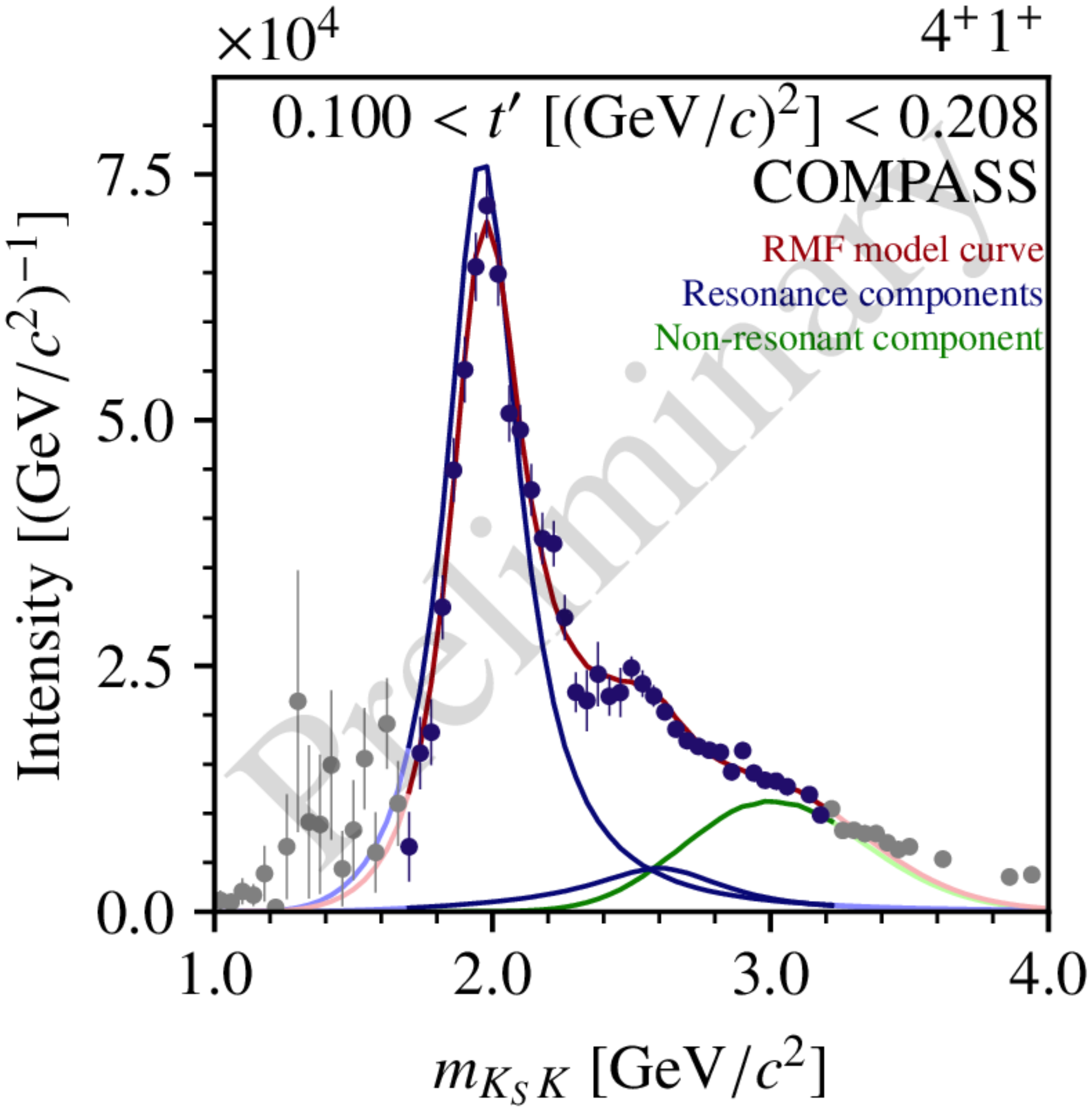

The $J^{PC} = 4^{++}$ Sector in $\omega\pi^-\pi^0$

$a_4(1970)$:

- Also measured in the $\omega\pi^-\pi^0$ final state:

$$m_0 = 1973 \pm 3\ {}^{+15}_{-8}\ \text{MeV}/c^2$$
$$\Gamma_0 = 311 \pm 8\ {}^{+10}_{-46}\ \text{MeV}/c^2$$

- No clear resonance signal at higher masses

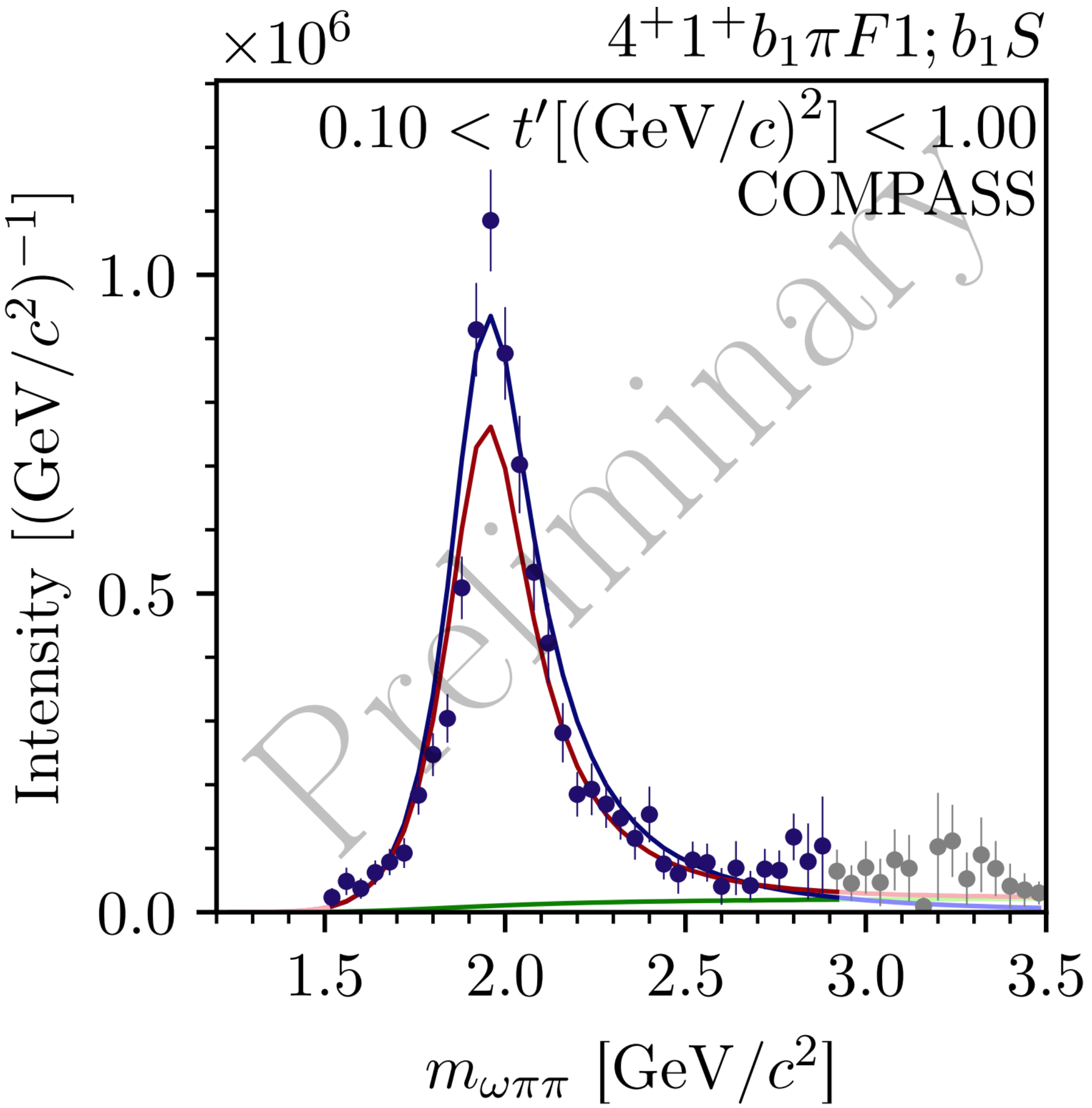

The $J^{PC} = 4^{++}$ Sector in $K_S^0 K^-$

a_4':

- Evidence for a higher state around 2.6 GeV/c^2

$$\boxed{\begin{aligned} m_0 &= 2608 \pm 9\,^{+5}_{-38}\ \mathrm{MeV}/c^2 \\ \Gamma_0 &= 609 \pm 22\,^{+35}_{-311}\,\mathrm{MeV}/c^2 \end{aligned}}$$

- Previous experiments claim such states around 2.25 GeV/c^2

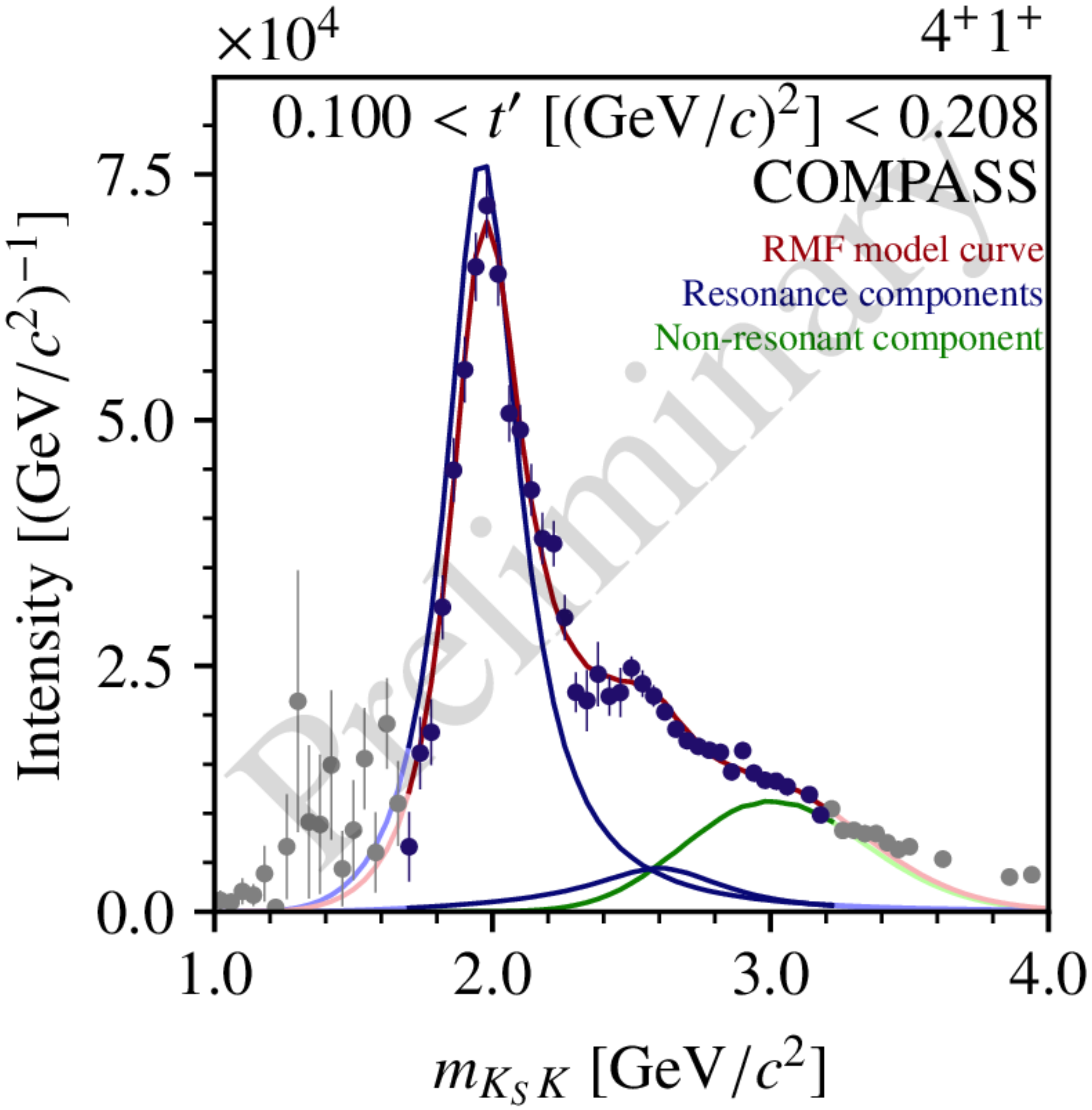

cf Particle Data Group, Phys. Rev. D **110**, 030001 (2024)

The $J^{PC} = 6^{++}$ Sector in $K_S^0 K^-$

$a_6(2450)$:

- Strong evidence for an a_6 state around $2.5\ \mathrm{GeV}/c^2$

$$m_0 = 2430 \pm 9\ {}^{+21}_{-25}\ \mathrm{MeV}/c^2$$
$$\Gamma_0 = 523 \pm 22\ {}^{+39}_{-119}\ \mathrm{MeV}/c^2$$

- Previously claimed only by Cleland et al., in $K_S^0 K^-$

Cleland et al., Nucl. Phys. B208 (1982) 228-261

- We are in agreement with their measurement

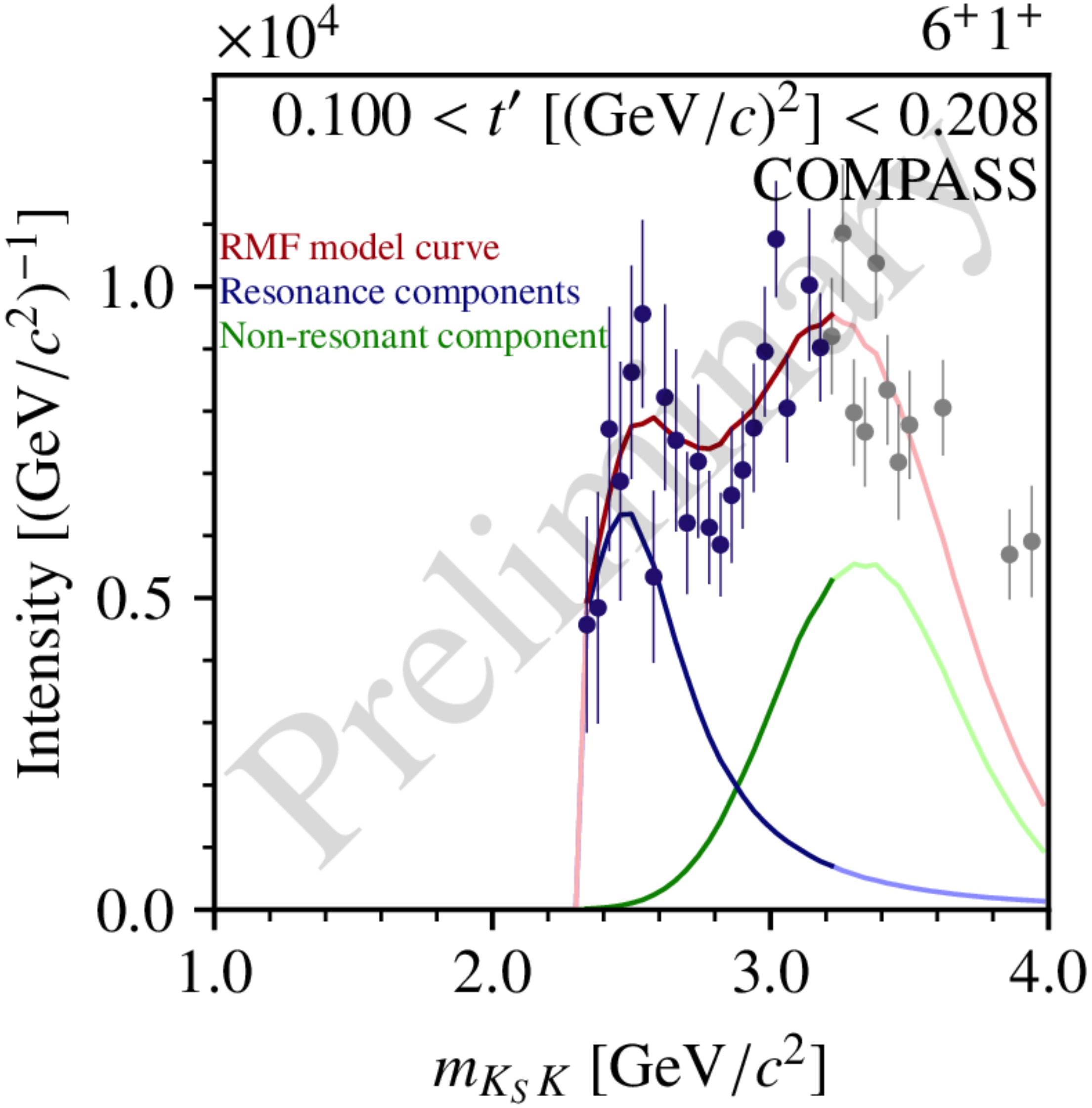

The $J^{PC} = 6^{++}$ Sector in $\omega\pi^-\pi^0$

$a_6(2450)$:

- Also clear signal in $\omega\pi^-\pi^0$

$$m_0 = 2558 \pm 31\,^{+12}_{-73}\ \mathrm{MeV}/c^2$$
$$\Gamma_0 = 600 \pm 90\,^{+60}_{-170}\ \mathrm{MeV}/c^2$$

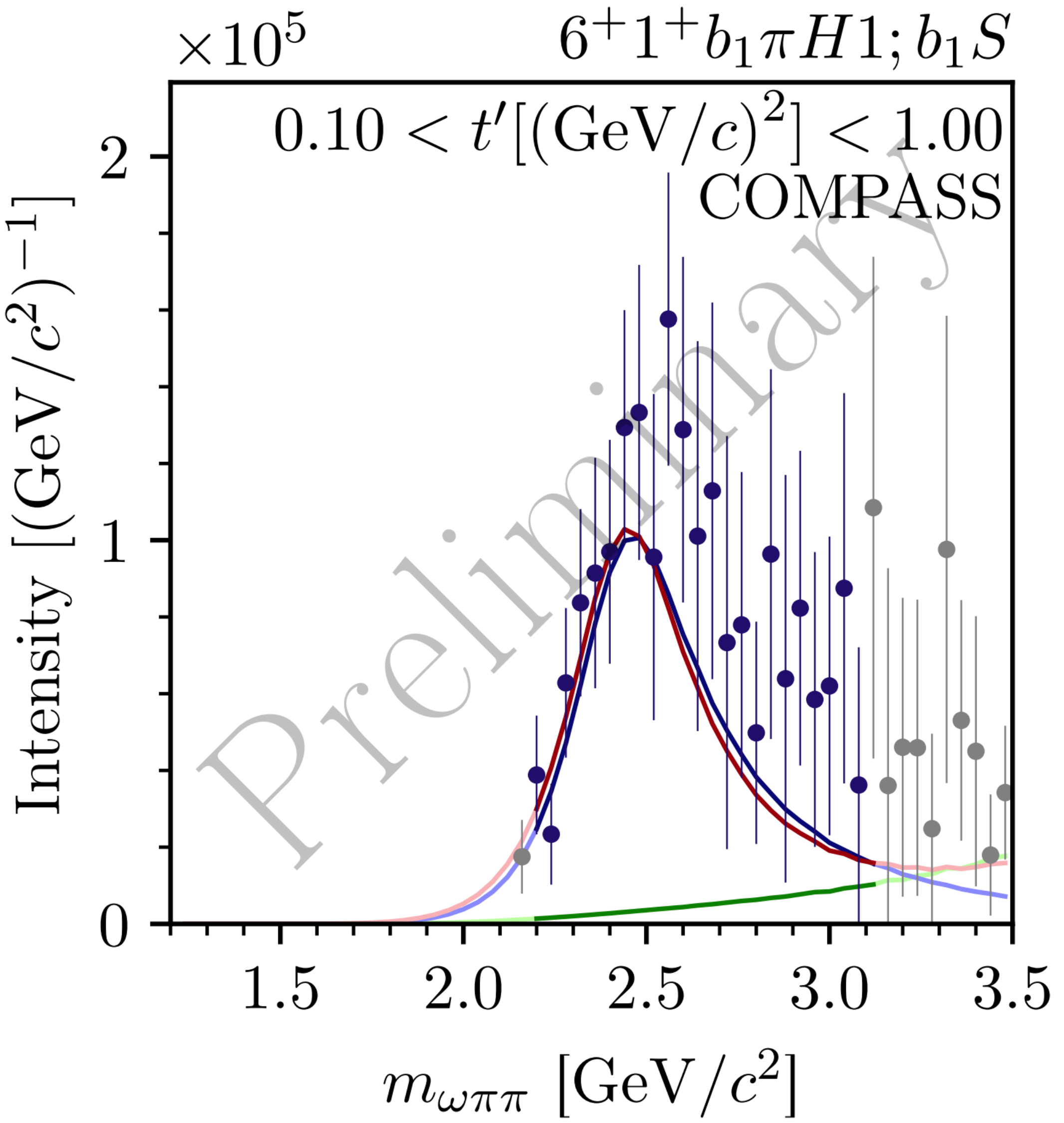

The Spin-Exotic $\pi_1(1600)$

QCD allows for states beyond $q\bar{q}$ (tetraquarks, molecules, hybrids, glueballs)

- Models and lattice QCD predict the lightest hybrid meson to have
  - $\boldsymbol{J^{PC} = 1^{-+}}$ quantum numbers, and
  - a dominant decay into $\boldsymbol{b_1(1235)\,\pi}$

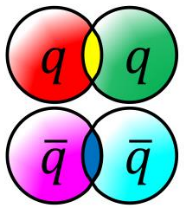

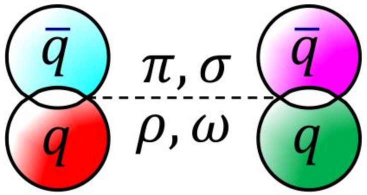

→ Spin-exotic meson (QN not possible for $q\bar{q}$)

→ measurable at COMPASS e.g. via $\boldsymbol{b_1(1235)\,\pi \to \omega\pi^-\pi^0}$

- COMPASS has a $\sim 5\times$ larger dataset for $\omega\pi^-\pi^0$ reactions than previous experiments
- Complement existing $\pi_1(1600)$ COMPASS measurements in $\eta^{(\prime)}\pi^-$ and $\pi^-\pi^-\pi^+$

from: Ketzer, Grube, Ryabchikov, Prog. Part. Nucl. Phys. 113 (2020) 103755

The $J^{PC} = 1^{-+}$ Sector in $\omega\pi^-\pi^0$

$\boldsymbol{\pi_1(1600)}$:

- Clear signal of a spin-exotic state around 1.6 GeV/c^2

$$m_0 = 1723 \pm 6\,^{+37}_{-14}\ \mathrm{MeV}/c^2$$
$$\Gamma_0 = 336 \pm 10\,^{+96}_{-33}\ \mathrm{MeV}/c^2$$

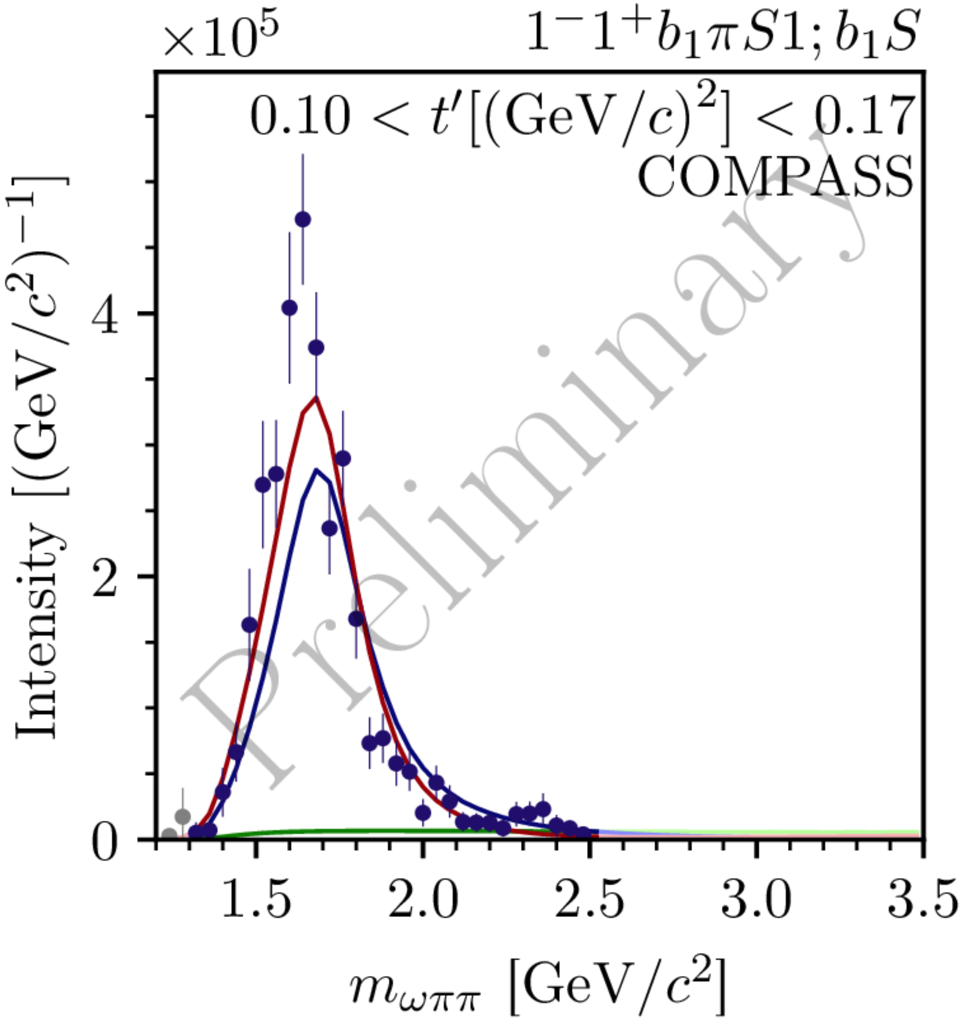

The $J^{PC} = 1^{-+}$ Sector in $\omega\pi^-\pi^0$

$\boldsymbol{\pi_1(1600)}$:

- Clear signal of a spin-exotic state around 1.6 GeV/c^2

$$m_0 = 1723 \pm 6\,^{+37}_{-14}\ \mathrm{MeV}/c^2$$
$$\Gamma_0 = 336 \pm 10\,^{+96}_{-33}\ \mathrm{MeV}/c^2$$

- No indication for an excited $\pi_1(2015)$ state (claimed by BNL E852 in $\omega\pi^-\pi^0$)

Lu et al., *Phys.Rev.Lett.* 94 (2005) 032002

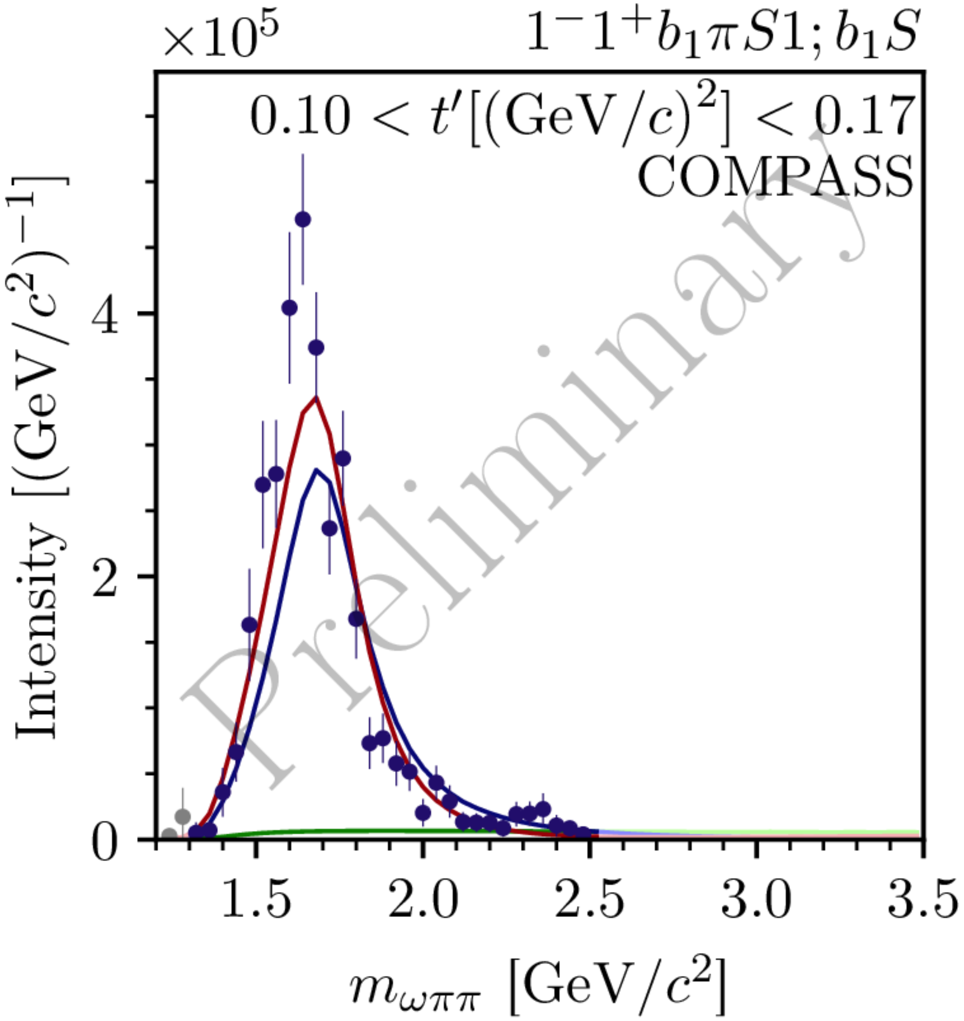

The $J^{PC} = 1^{-+}$ Sector in $\omega\pi^-\pi^0$

$\pi_1(1600)$:

- Clear signal of a spin-exotic state around 1.6 GeV/c^2

$$m_0 = 1723 \pm 6\ ^{+37}_{-14}\ \text{MeV}/c^2$$
$$\Gamma_0 = 336 \pm 10\ ^{+96}_{-33}\ \text{MeV}/c^2$$

- No indication for an excited $\pi_1(2015)$ state (claimed by BNL E852 in $\omega\pi^-\pi^0$)

Lu et al., *Phys.Rev.Lett.* 94 (2005) 032002

Decay modes:

- Predicted dominant decay into $b_1(1235)\pi$
- Also measured in $\rho\omega$ decay

→ First observation of this decay

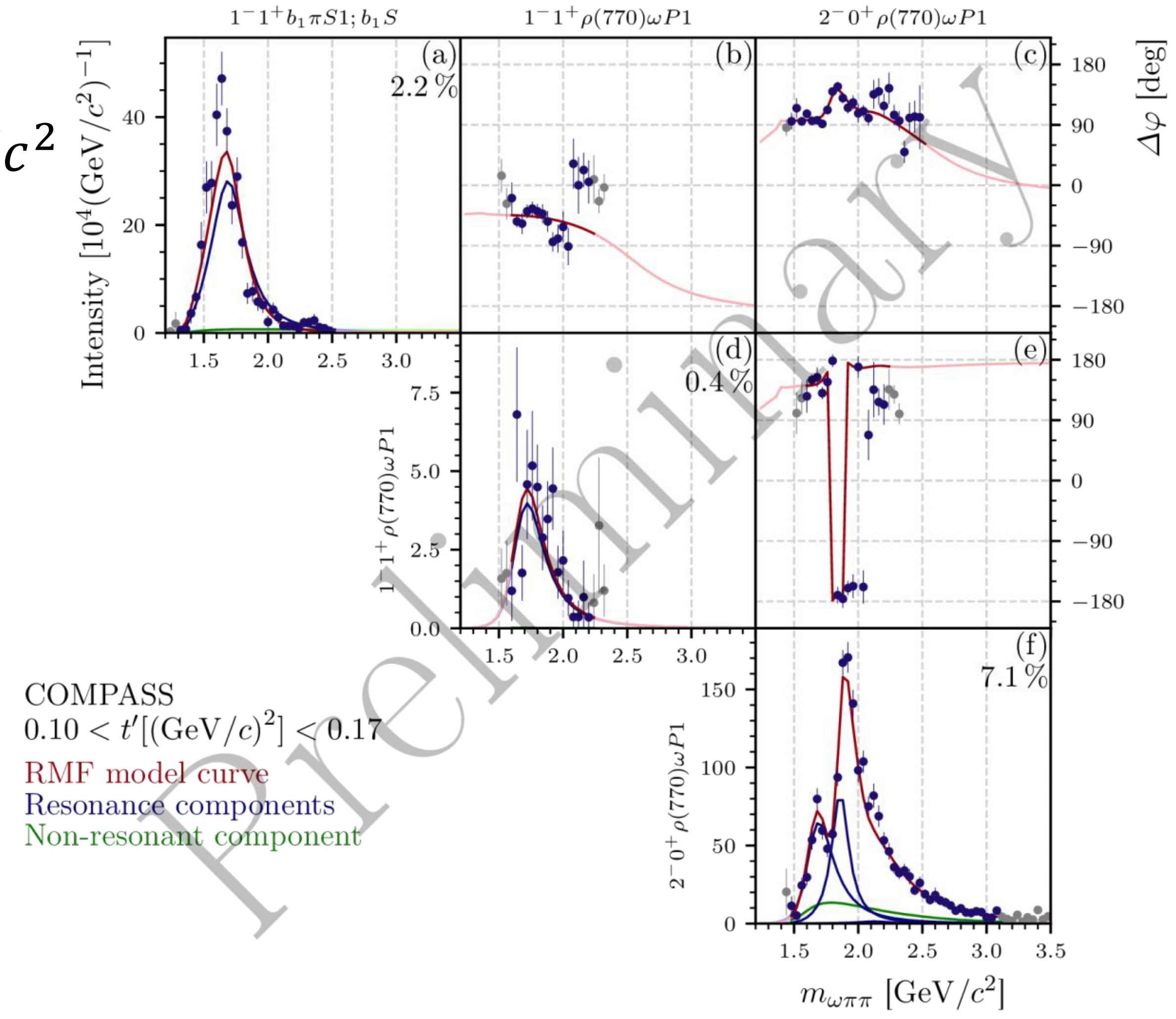

Conclusion

- The COMPASS experiment has the world‘s largest datasets for many light-meson final states
- Partial-wave analyses allow to measure resonances with high precision

- 6 a_J mesons are measured up to high invariant masses in $K_S^0 K^-$
- Second observation of the $a_6(2450)$ state

- Resonance parameters of 11 states extracted in $\omega\pi^-\pi^0$ ($a_3, \pi_4, a_6, \ldots$)
- New measurements of the $\pi_1(1600)$ in $b_1\pi^- \rightarrow \omega\pi^-\pi^0$
  (and in $f_1\pi^- \rightarrow \eta 3\pi$, see D. Spülbeck‘s talk on Saturday)
- Multiple decay channels measured, first observation of $\rho(770)\omega$

- Many other analyses in progress (H. Pekeler‘s talk on Saturday)

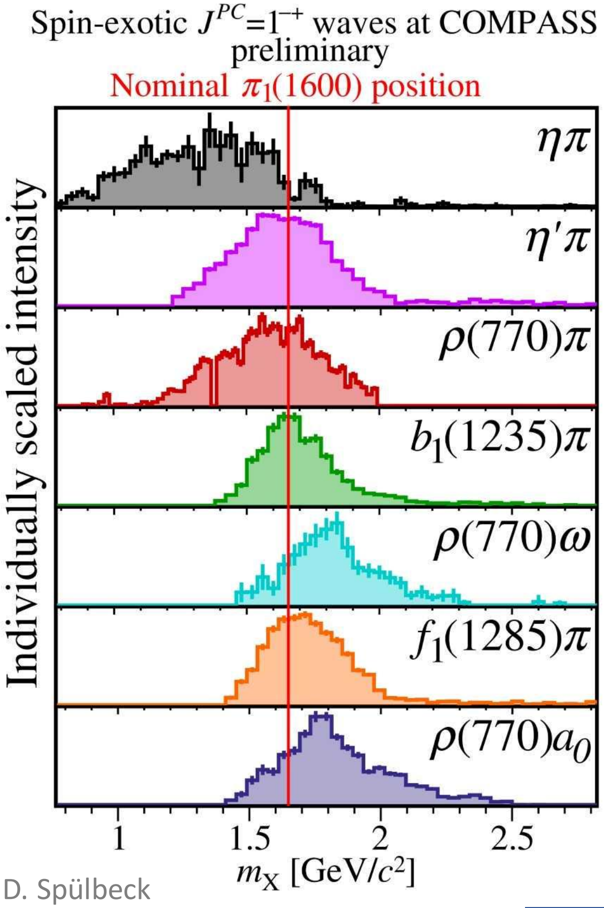

Courtesy of D. Spülbeck

BACKUP

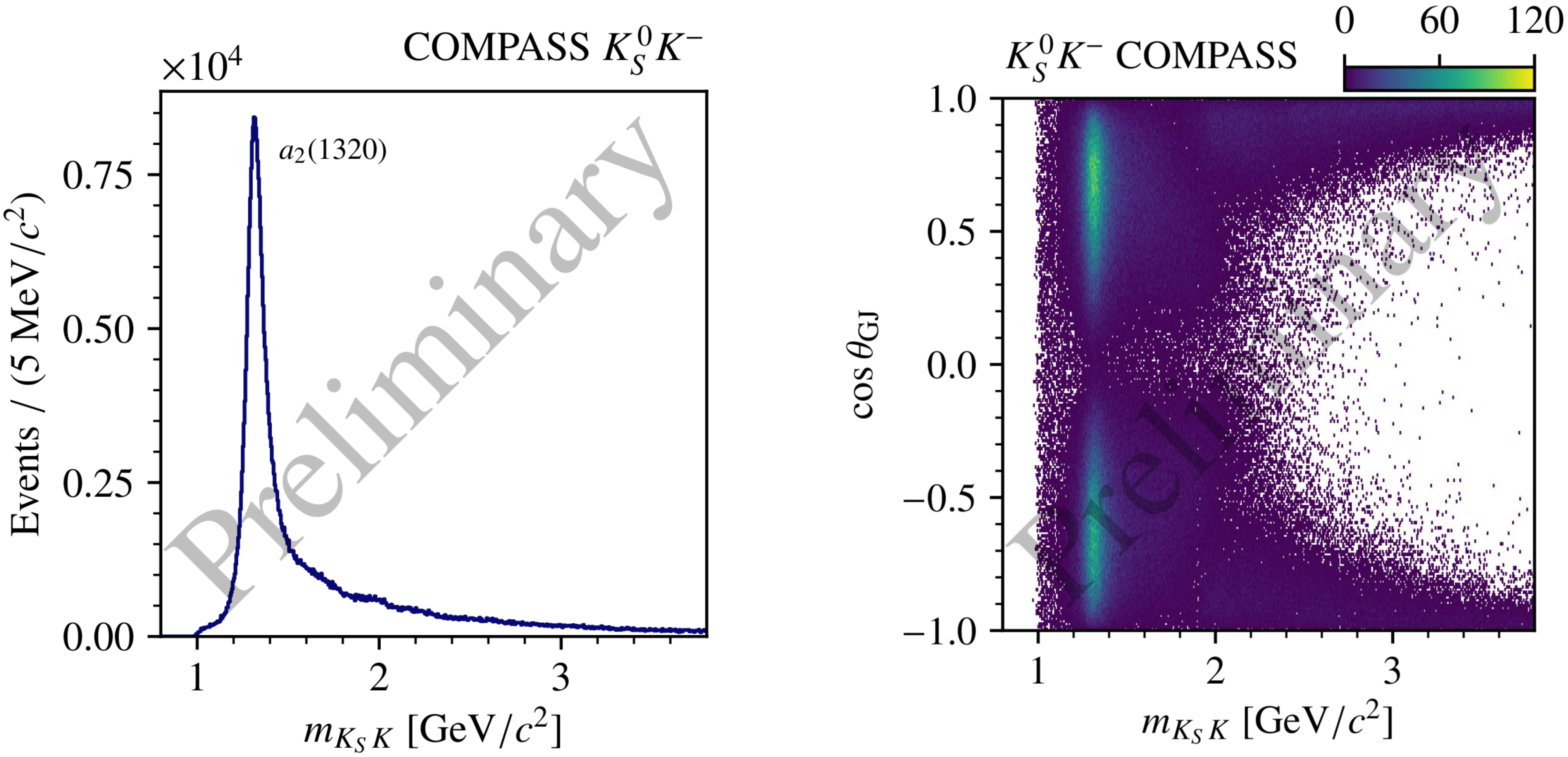
COMPASS $K_S^0 K^-$
$\times 10^4$
$a_2(1320)$
Events / (5 MeV/c^2)
0.00
0.25
0.50
0.75
1
2
3
$m_{K_S K}$ [GeV/c^2]
Preliminary
0
60
120
$K_S^0 K^-$ COMPASS
$\cos\theta_{GJ}$
1.0
0.5
0.0
−0.5
−1.0
1
2
3
$m_{K_S K}$ [GeV/c^2]
Preliminary

Ambiguities in the Partial-Wave Decomposition

For any final state with **two spinless** particles ($\pi\pi, KK, \eta\pi$, ...):

- Decomposition of intensity into $\{T_{J,M}\}$ is not **unique**

  → Several sets of $\{T_{J,M}\}$ lead to the **same** $\boldsymbol{I(\theta,\phi)}$ in each (m_{KK}, t') bin

$$I(\theta,\phi) = \left|\sum_{J,M} T_{J,M}^{(1)}\, Y_J^M(\theta,\phi)\right|^2 = \left|\sum_{J,M} T_{J,M}^{(2)}\, Y_J^M(\theta,\phi)\right|^2$$

- The fit cannot distinguish between the **mathematically equivalent** solutions!

Chung, PRD 56 7299–7316 (1997)

Barrelet, *Nuov Cim A* **8**, 331–371 (1972)

Ambiguities in the Partial-Wave Decomposition

$$I(\theta,\phi) = \left|\sum_{J,M} T_{J,M}\, Y_J^M(\theta,\phi)\right|^2$$

Assume strong dominance of $|M| = 1$ *

- Pomeron exchange dominant $\rightarrow M \neq 0$
- Higher $|M|$ suppressed

*using reflectivity basis for ψ_{JM} :
doi.org/10.1103/PhysRevD.11.633

Ambiguities in the Partial-Wave Decomposition

$$I(\theta,\phi) = \left|\sum_J T_J\, Y_J^1(\theta,\phi)\right|^2$$

Assume strong dominance of $|M| = 1$ *

- Pomeron exchange dominant $\rightarrow M \neq 0$
- Higher $|M|$ suppressed

*using reflectivity basis for ψ_{JM} :
doi.org/10.1103/PhysRevD.11.633

Ambiguities in the Partial-Wave Decomposition

$$I(\theta,\phi) = \left|\sum_J T_J\, Y_J^1(\theta,\phi)\right|^2 = \underbrace{\left|\sum_J T_J\, Y_J^1(\theta,0)\right|}_{\boldsymbol{a(\theta)}}^2 \;|\sin\phi|^2$$

$$\boxed{Y_J^1(\theta,0) = \sum_{j=0}^{J-1} y_j \tan^{2j}\theta}$$

Polynomial in $\tan^2\theta$

$$a(\theta) = \sum_{j=0}^{J_{\max}-1} c_j(\{T_J\})\,\tan^{2j}(\theta) = c(\{T_J\}) \prod_{k=1}^{J_{\max-1}} \left(\tan^2(\theta) - \boldsymbol{r}_k(\{T_J\})\right)$$

root decomposition

“Barrelet zeros”

$$\{T_J{}'\} \neq \{T_J\}$$

$$\{c_j{}'\}$$

$$= c^2 \prod_{k=1}^{J_{\max-1}} |\tan^2(\theta) - \boldsymbol{r}_k|^2\;|\sin\phi|^2 = c^2 \prod_{k=1}^{J_{\max-1}} |\tan^2(\theta) - \boldsymbol{r}_k^*|^2\;|\sin\phi|^2$$

Study of the Ambiguities

I. Continuous amplitude model

How do the ambiguous solutions look like (**continuity, signals, …**)?

- Create an amplitude model for four partial waves
- Sample points in m_{KK} and calculate ambiguous solutions

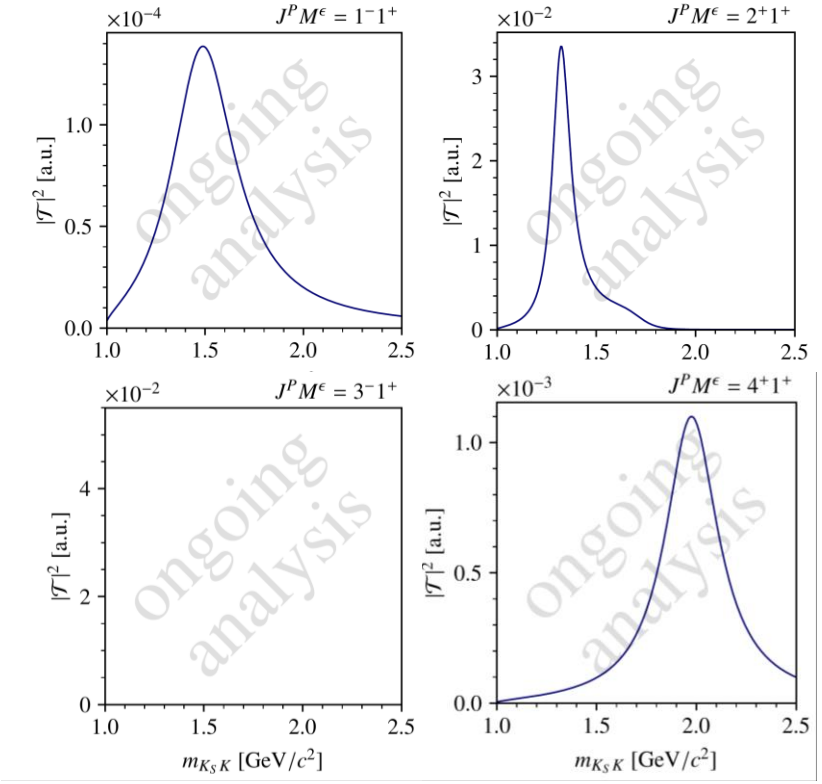

Continuous Amplitude Model

I. Continuous amplitude model $\boxed{N_a = 3}$

How do the ambiguous solutions look like?

- Create an amplitude model for four partial waves
- Sample points in m_{KK} and calculate ambiguous solutions

- Ambiguous intensities are also continuous
- Not all solutions are different from each other!
- Highest-spin (4^{++}) intensity is invariant!

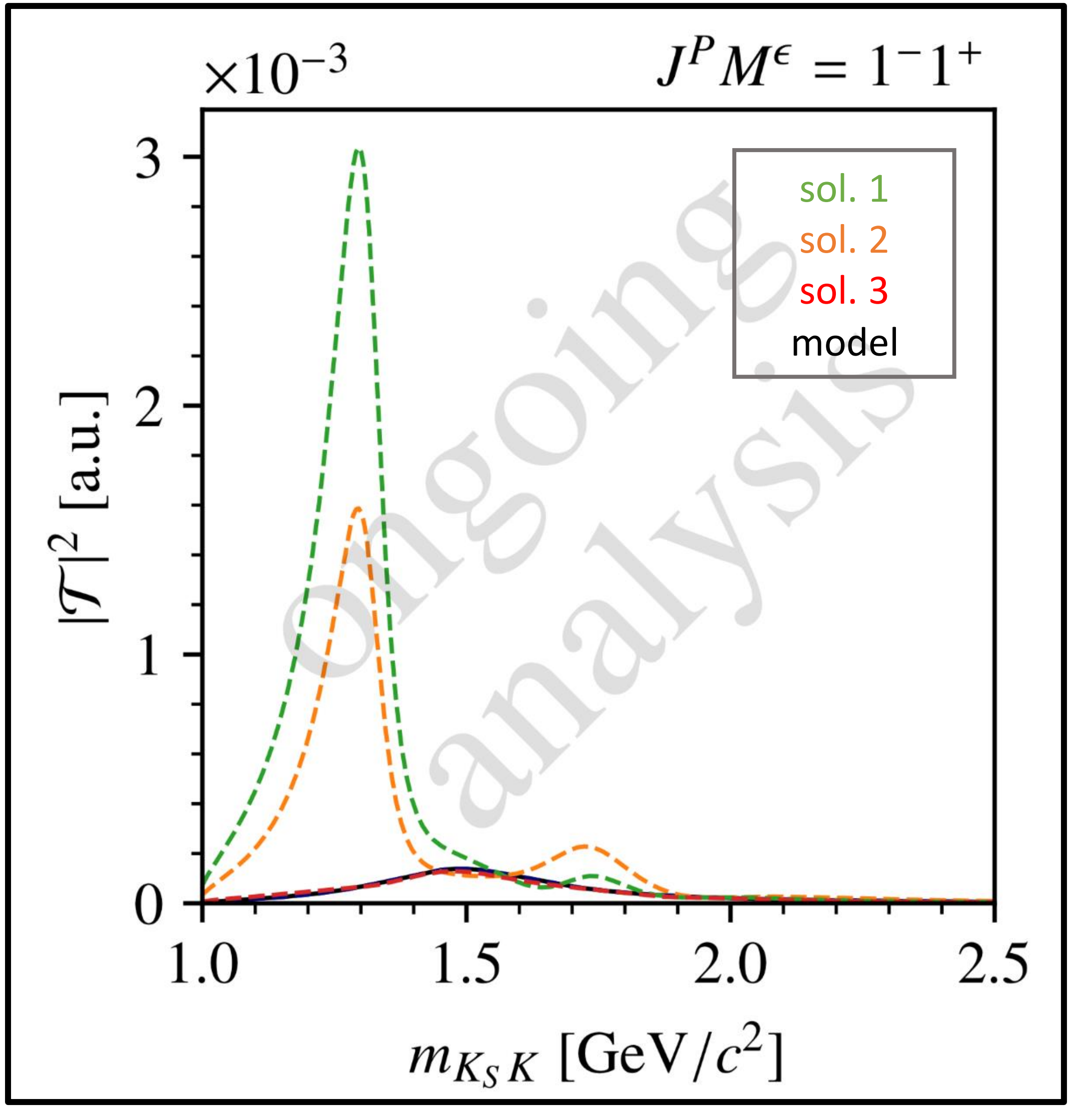

Continuous Amplitude Model

I. Continuous amplitude model $\boxed{N_a = 3}$

How do the ambiguous solutions look like?

- Create an amplitude model for four partial waves
- Sample points in m_{KK} and calculate ambiguous solutions

- Ambiguous intensities are also continuous
- Not all solutions are different from each other!
- Highest-spin (4^{++}) intensity is invariant!

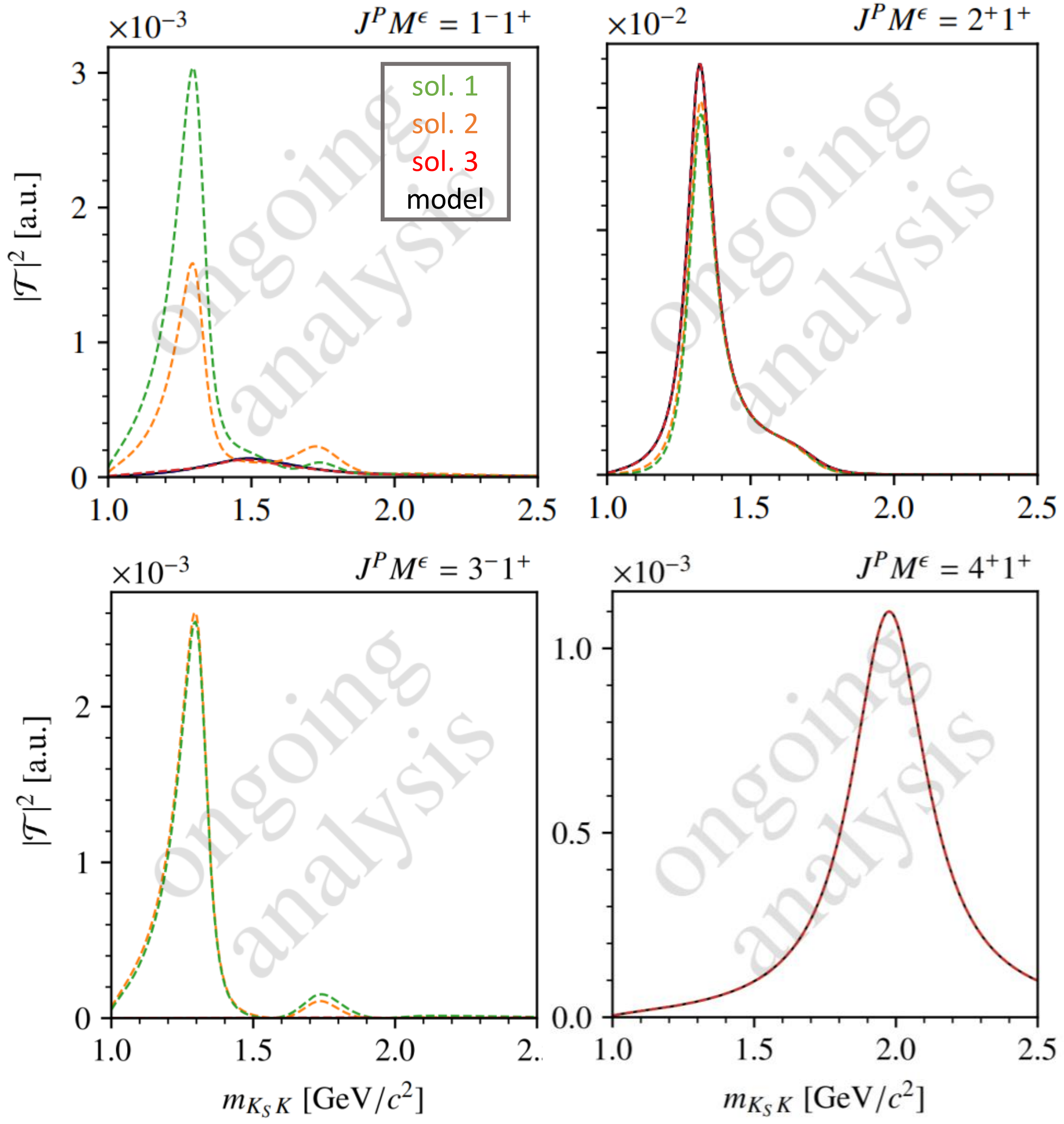

Partial-Wave Decomposition Fits on Pseudodata

II. Finite pseudo-data

- reality: **finite data** and **amplitudes unknown**
- generate pseudo-data according to model
- perform a partial-wave decomposition fit

→ 3000 attempts with random start values

- 4^{++} intensity is still invariant!
- Overall, amplitude values found by the fit follow the calculated distributions
- Not all solutions are found in each m_X bin

→ PWD fit distorts the intensity distribution!

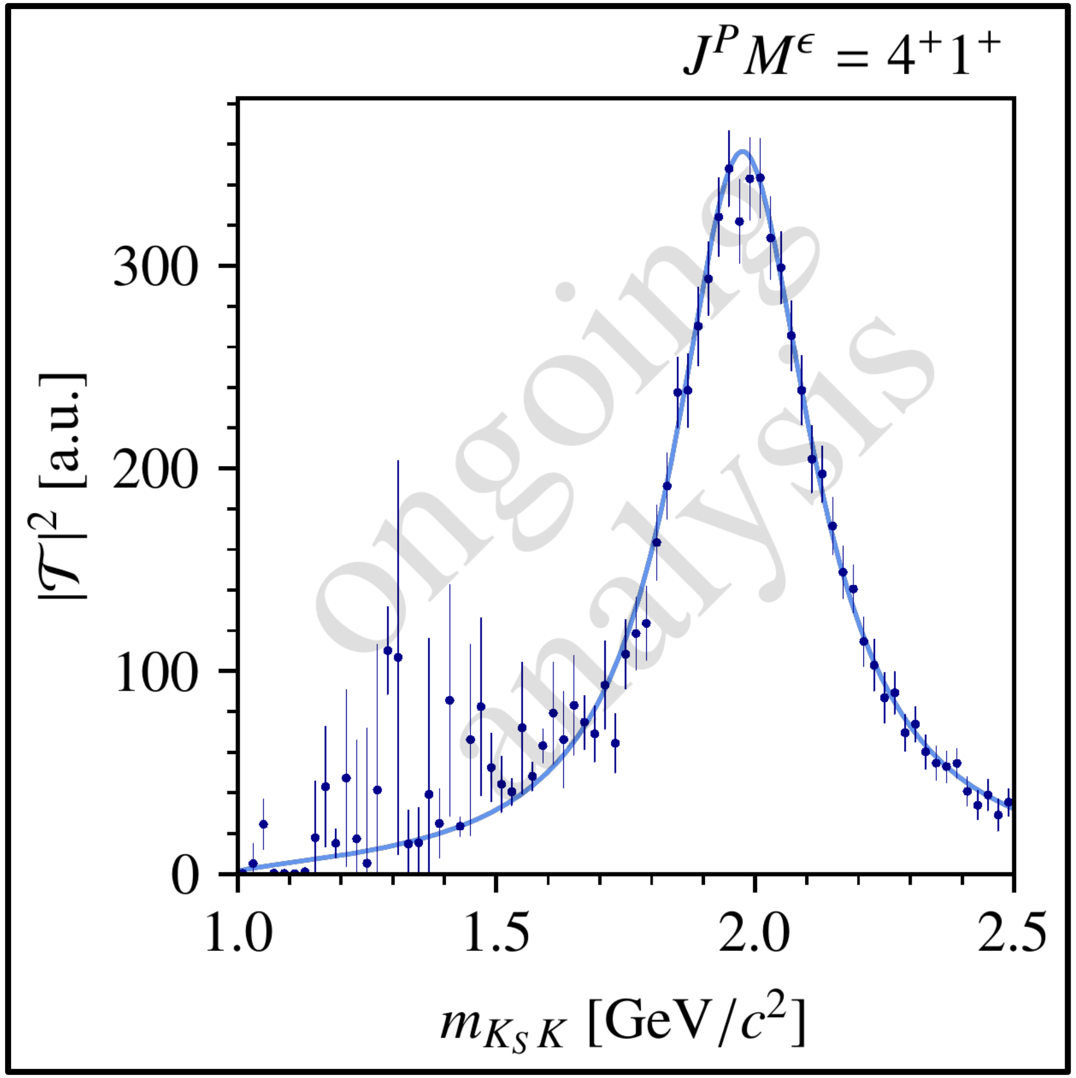

Partial-Wave Decomposition Fits on Pseudodata

II. Finite pseudo-data

- reality: **finite data** and **amplitudes unknown**
- generate pseudo-data according to model
- perform a partial-wave decomposition fit

→ 3000 attempts with random start values

- 4^{++} intensity is still invariant!
- Overall, amplitude values found by the fit follow the calculated distributions
- Not all solutions are found in each m_{KK} bin

→ PWD fit distorts the intensity distribution!

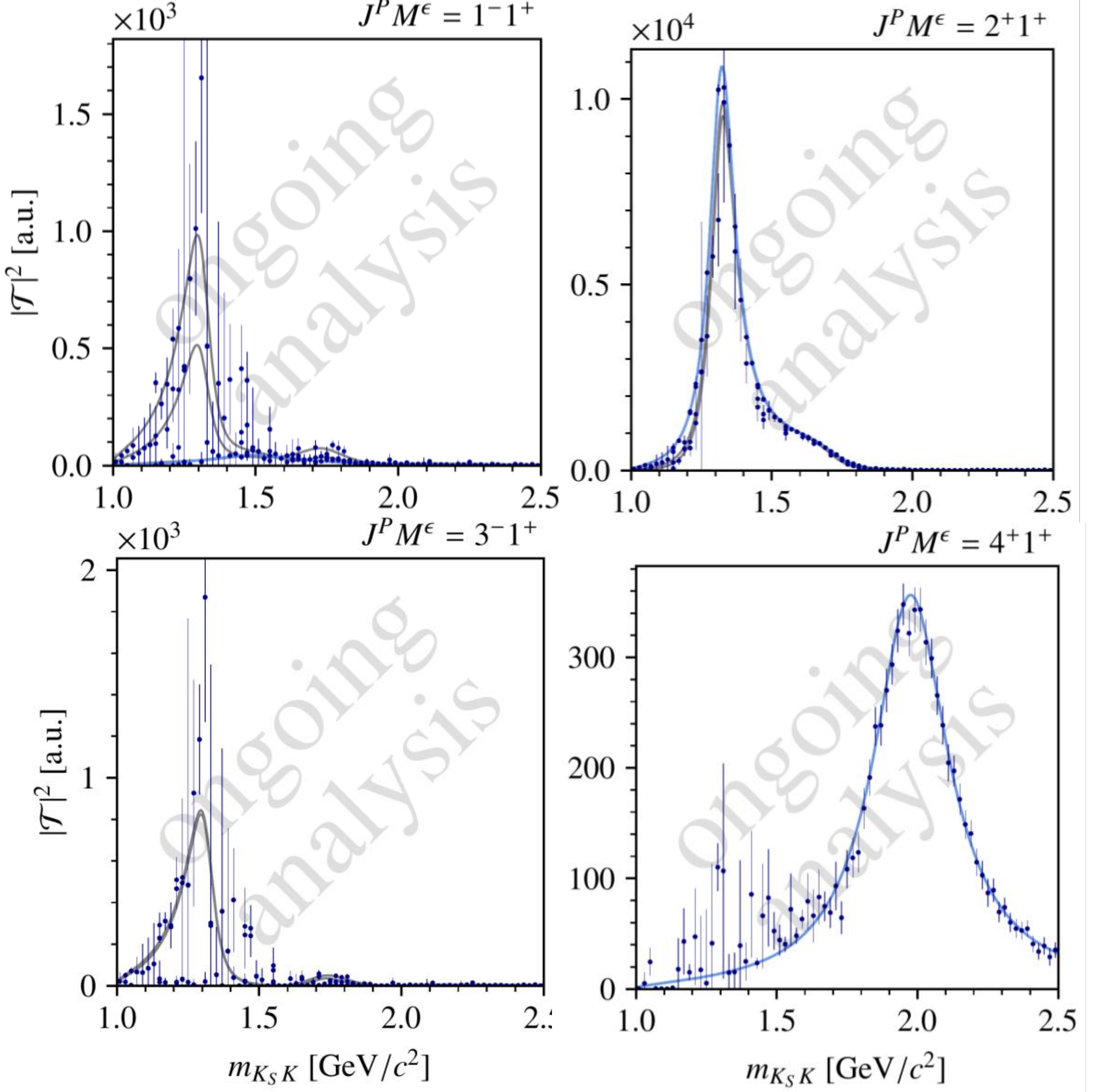

Partial-Wave Decomposition Fits on Pseudodata

II. Finite pseudo-data

- reality: **finite data** and **amplitudes unknown**
- generate pseudo-data according to model
- perform a partial-wave decomposition fit

→ 3000 attempts with random start values

- 4^{++} intensity is still invariant!
- Overall, amplitude values found by the fit follow the calculated distributions
- Not all solutions are found in each m_{KK} bin

→ PWD fit distorts the intensity distribution!

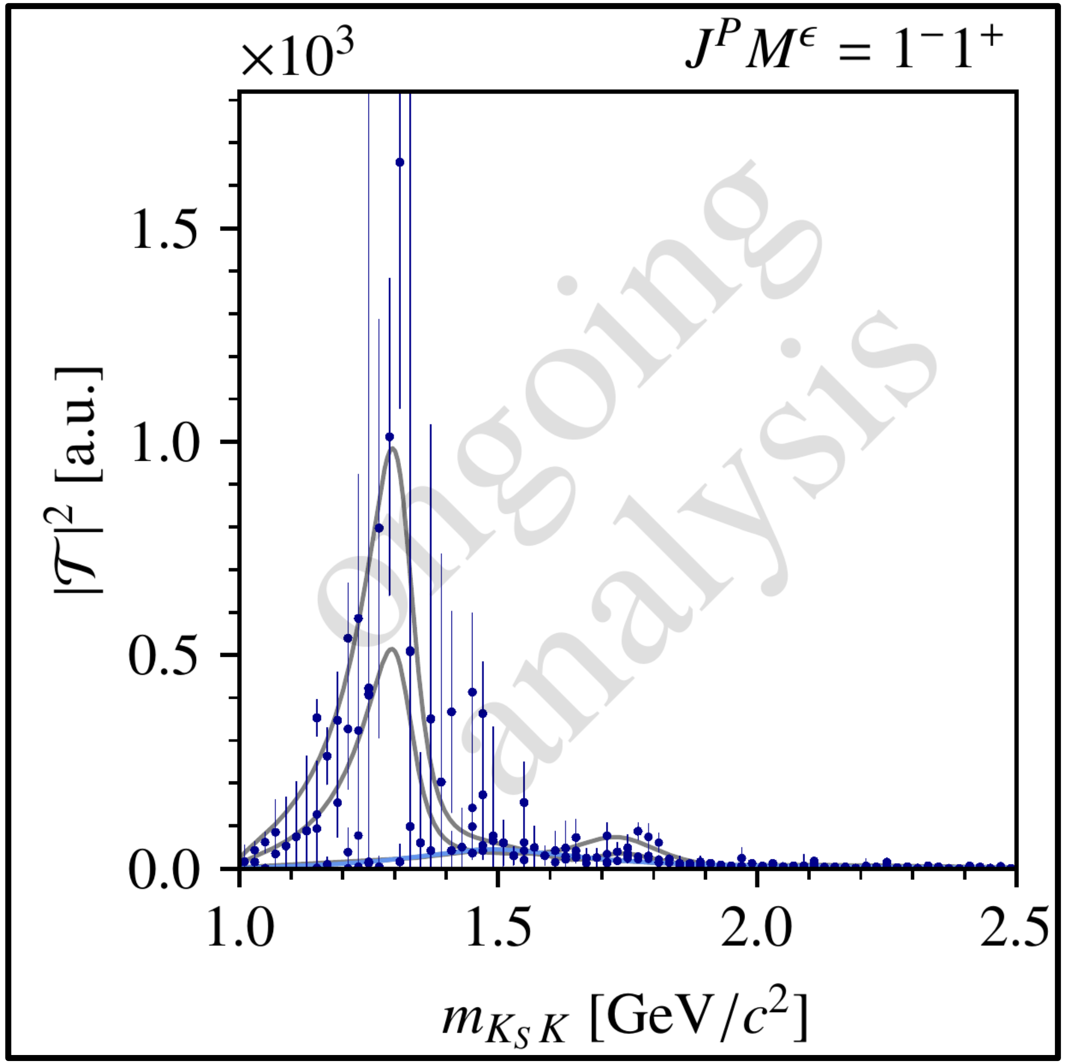

Reducing the Ambiguities

- Intensity of highest-spin wave is unaffected by ambiguities
- Remove one wave with $J < J_{\max}$ → **resolves ambiguities**

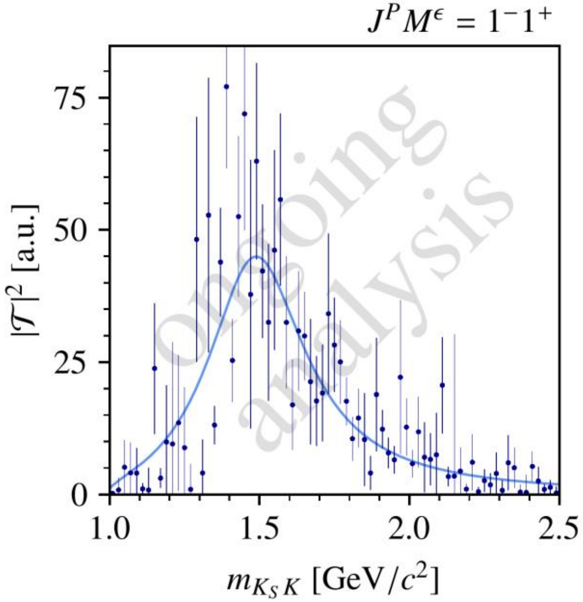

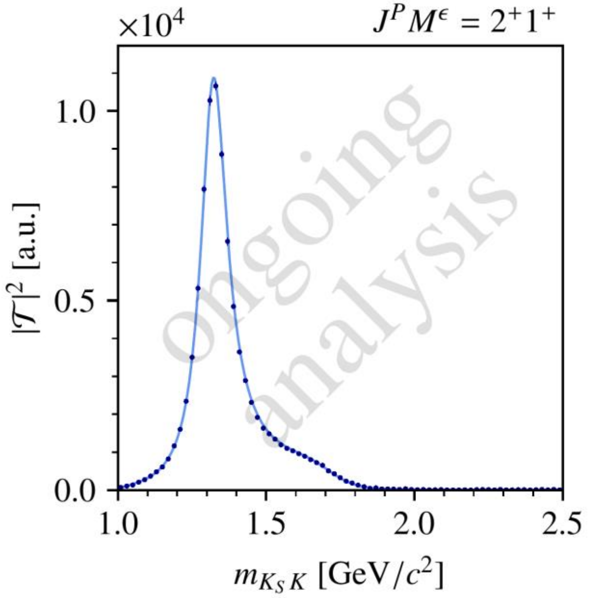

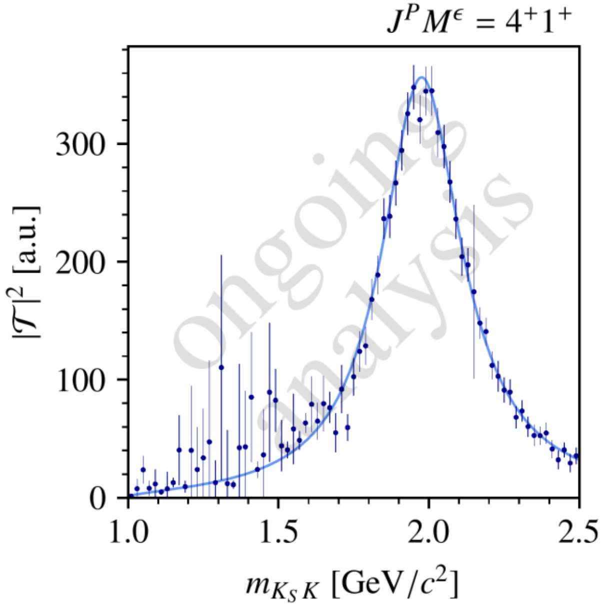

At COMPASS: **odd-spin waves strongly suppressed**!

→ <u>assume no ambiguities in the decomposition!</u>

- Except: Two solutions in the phases of the partial waves

$$I(\theta,\phi) = \left|\sum_J T_J\, Y_J^1(\theta,\phi)\right|^2 = \left|\sum_J T_J^*\, Y_J^1(\theta,\phi)\right|$$

Agreement Between Model and Data

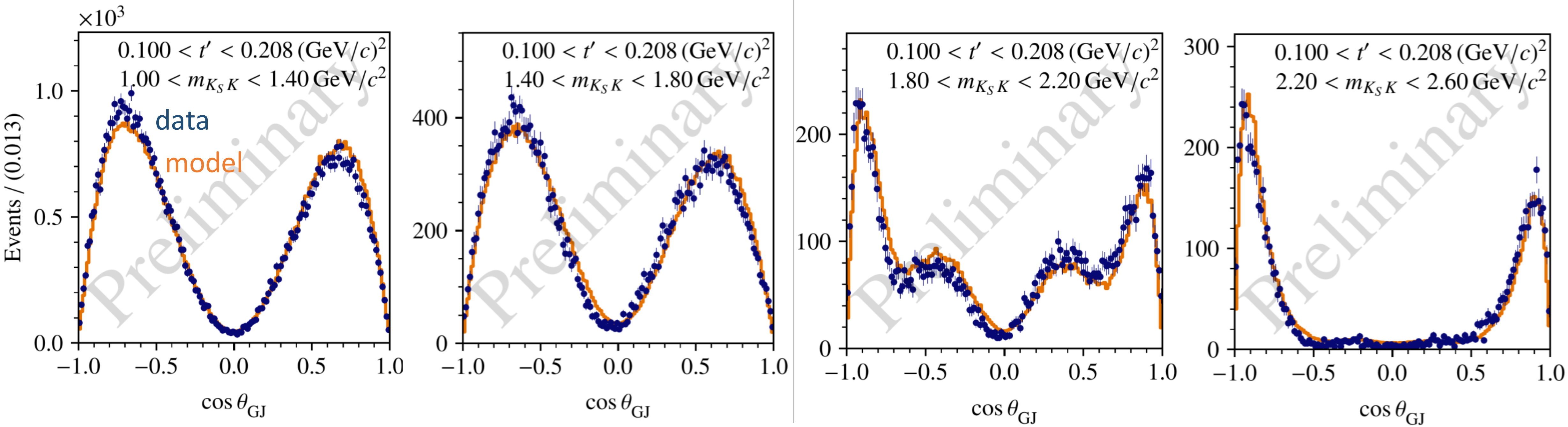

- Angular distributions as predicted by the PWA model after the fit vs real data
- Good agreement, but data exhibits larger asymmetry than predicted in the model

Adding an Odd-Spin Wave

How can we introduce asymmetry in the model?

- Effects of the detector acceptance
- Introduce partial wave(s) with odd spin J

$$\boxed{I^G J^{PC} = 1^+ 1^{--}}$$

- Cannot be produced via Pomeron exchange!

(but e.g. by ω exchange)

$\boldsymbol{\rho(1450)}$	$\boldsymbol{\rho(1700)}$
• $m = 1.47$ GeV	• $m = 1.73$ GeV
• $\Gamma = 0.40$ GeV	• $\Gamma = 0.25$ GeV

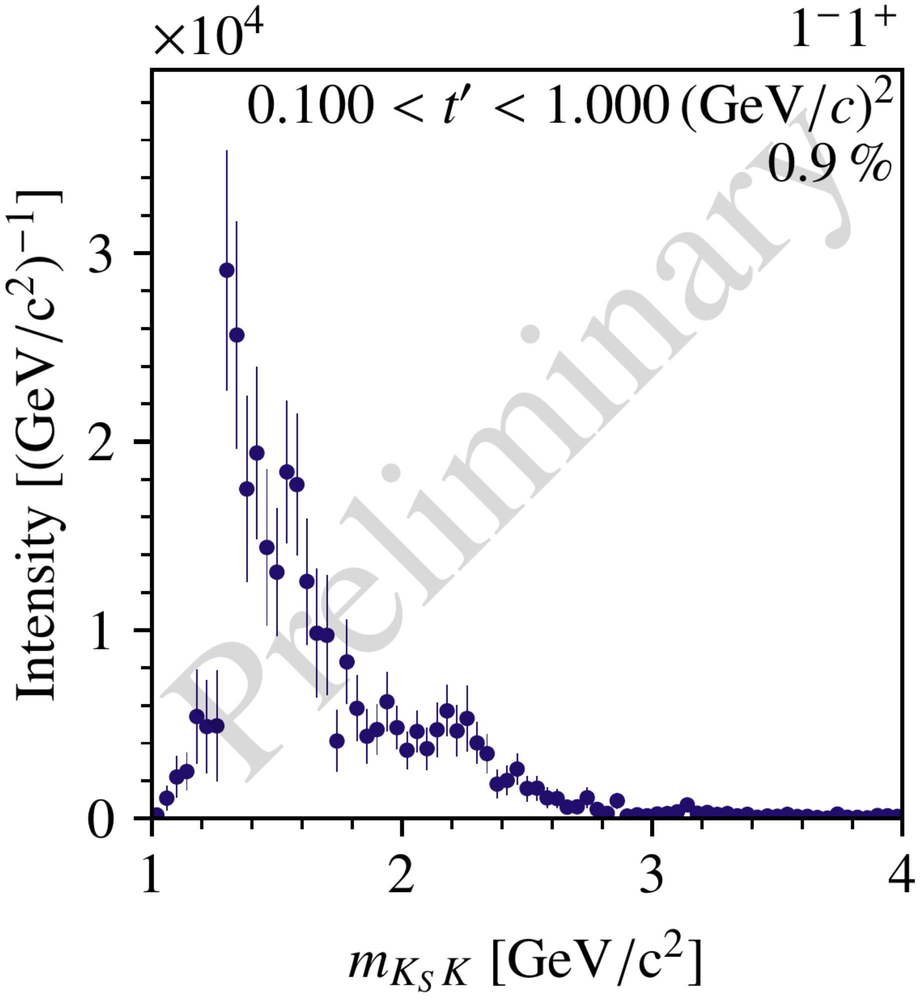

Agreement Between Model and Data II

Without 1^- wave

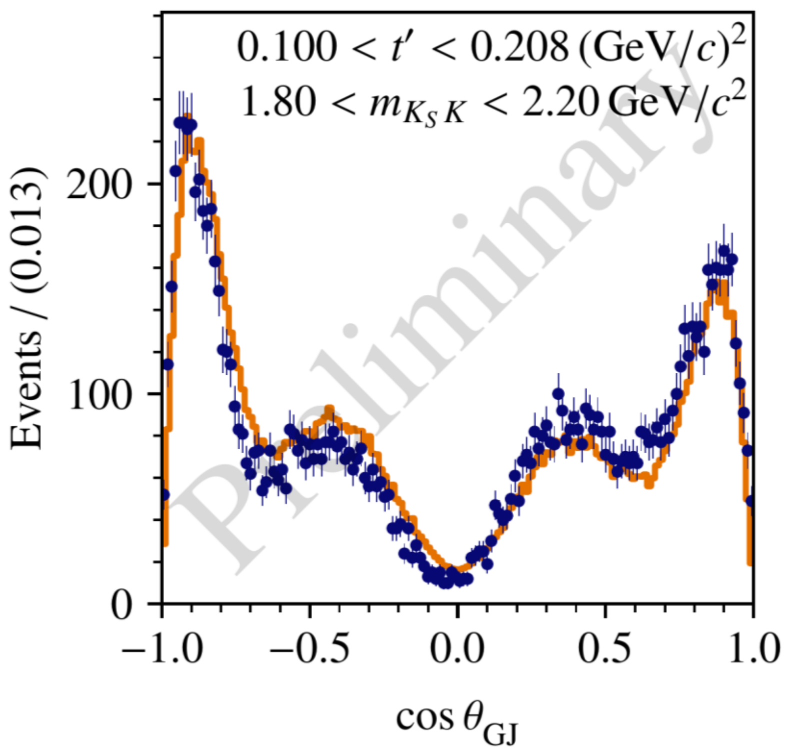

With 1^- wave

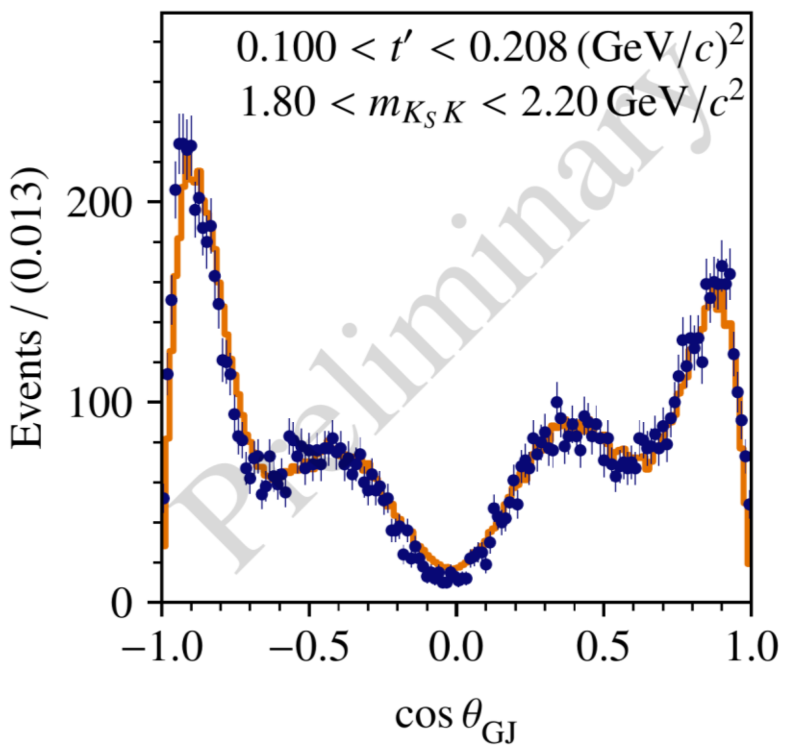

- Interference of $J = 1$ and even J could explain the forward/backward asymmetry

Resonance-Model Fit

Parameterize m_{KK}, t' dependence of $\boldsymbol{T_{JM}(m_{K_S K}, t')}$

In each partial wave:

$$\boldsymbol{T_{JM}(m_{K_S K}, t')} = \sum_{\mathbf{res.}\, i} c_i^{(JM)} D_i(m_{K_S K})$$

1. One or more resonances

→ Breit-Wigner amplitude(s) with fixed/dynamic width

$$D(m_{K_S K}; m_0, \Gamma_0) = \frac{m_0\, \Gamma_0}{m_0^2 - m_{K_S K}^2 - i[m_0 \Gamma(m_{K_S K})]}$$

$$\Gamma(m_{K_S K}) = \begin{cases} \Gamma_{\rho\pi}(m_{K_S K}) + \Gamma_{\eta\pi}(m_{K_S K}) & \text{for } a_2(1320) \\ \Gamma_0 & \text{else} \end{cases}$$

Resonance-Model Fit

Parameterize m_{KK}, t' dependence of $\boldsymbol{T_{JM}(m_{K_S K}, t')}$

In each partial wave: $$\boldsymbol{T_{JM}(m_{K_S K}, t')} = \sum_{\mathbf{res.}\, \boldsymbol{i}} c_i^{(JM)} D_i(m_{K_S K}) + \mathrm{BG}(m_{K_S K})$$

2. Background contributions

$$\exp[-b \cdot q^2(m_{K_S K})]$$

$$(m_{K_S K} - m_{\mathrm{thr}})^a \exp[-b \cdot q^2(m_{K_S K})],^{(*)}$$

(*) $b = e^c$

Resonance-Model Fit

Parameterize m_{KK}, t' dependence of $\boldsymbol{T_{JM}(m_{K_S K}, t')}$

In each partial wave: $$\boldsymbol{T_{JM}(m_{K_S K}, t')} = PS(m_{K_s K}, t') \left[\sum_{\mathbf{res.}\,\boldsymbol{i}} c_i^{(JM)} D_i(m_{K_S K}) + \mathrm{BG}(m_{K_S K}) \right]$$

3. Phase-space factors

$$PS(m_{K_s K}, t') = \sqrt{m_{K_S K} \cdot P_{\mathrm{prod}}(m_{K_S K}, t') \cdot I_{aa} \cdot F_J^2(q^2(m_{K_S K}))}$$

Production factor: $P_{\mathrm{prod}}(m_{K_S K}, t') = \left(\frac{s_0}{m_{K_S K}^2}\right)^{2\alpha_0 - 2\alpha' \cdot t' - 1}$

Phase space factor: $I_{aa} \cdot F_J^2(q^2(m_{K_S K}))$

The $K_S^0 K^-$ RMF

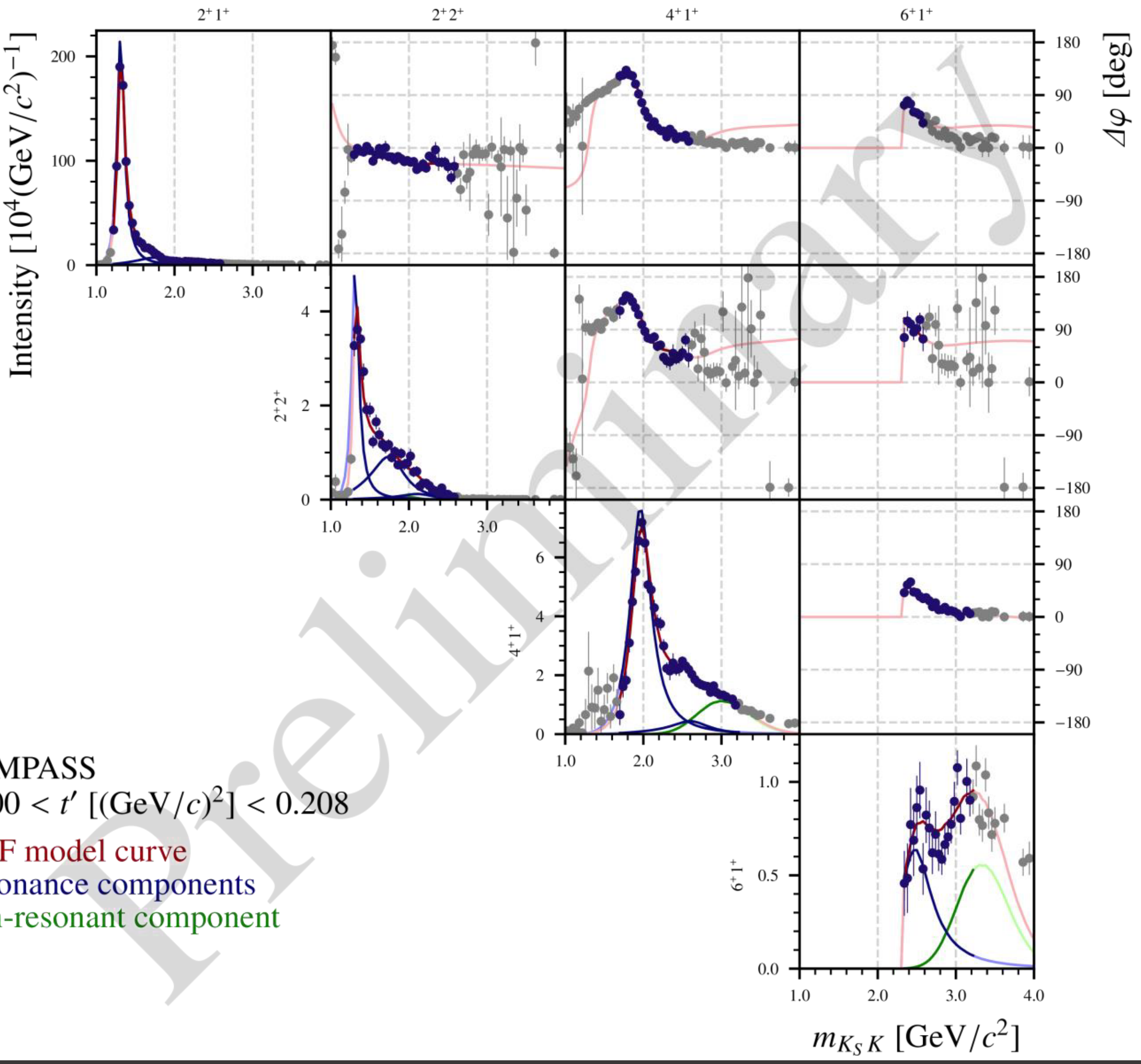

COMPASS
$0.100 < t'$ [$(\mathrm{GeV}/c)^2$] < 0.208

RMF model curve
Resonance components
Non-resonant component

The $J^{PC} = 2^{++}$ Sector in $K_S^0 K^-$

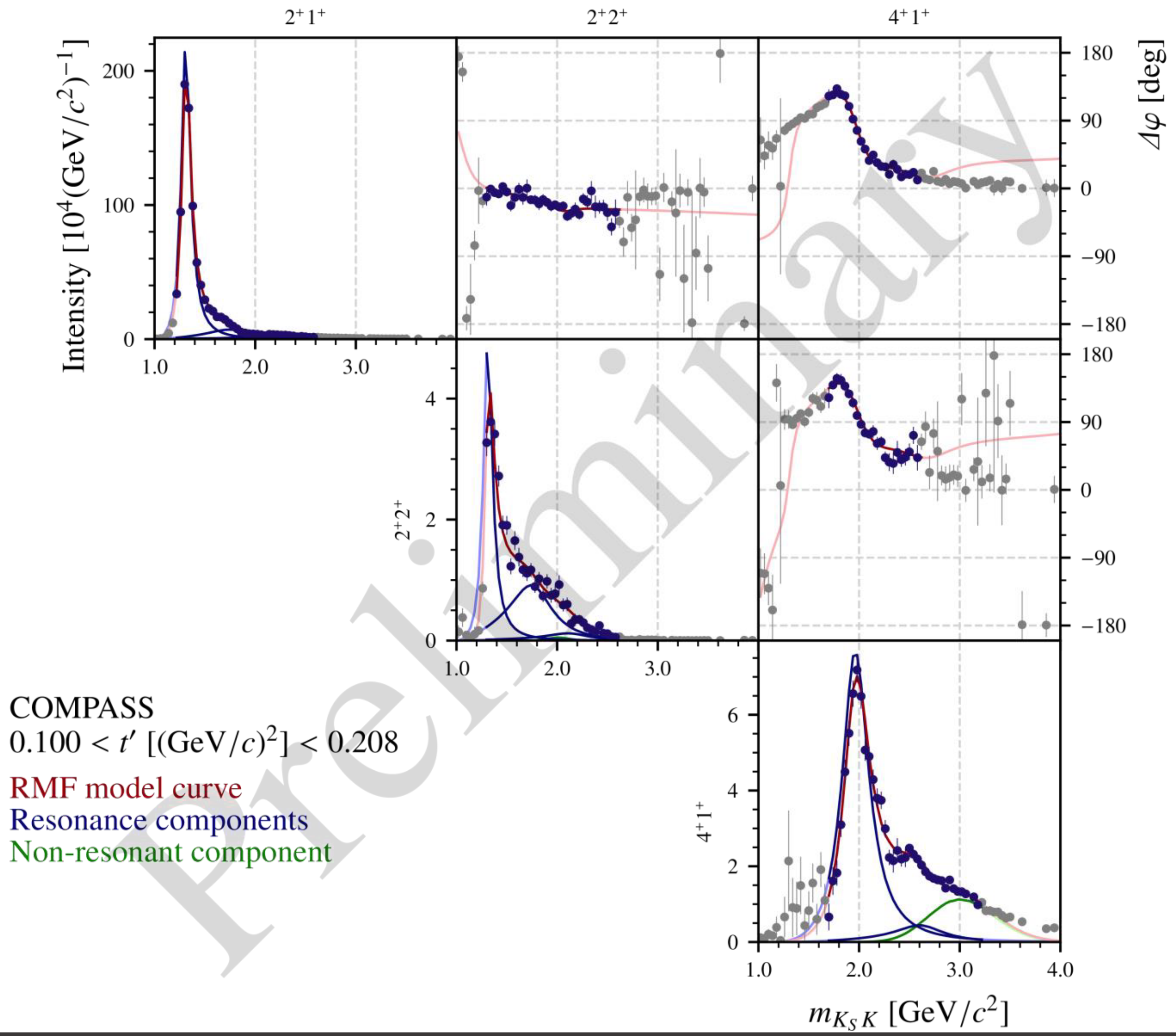

The $J^{PC} = 2^{++}$ Sector in $K_S^0 K^-$

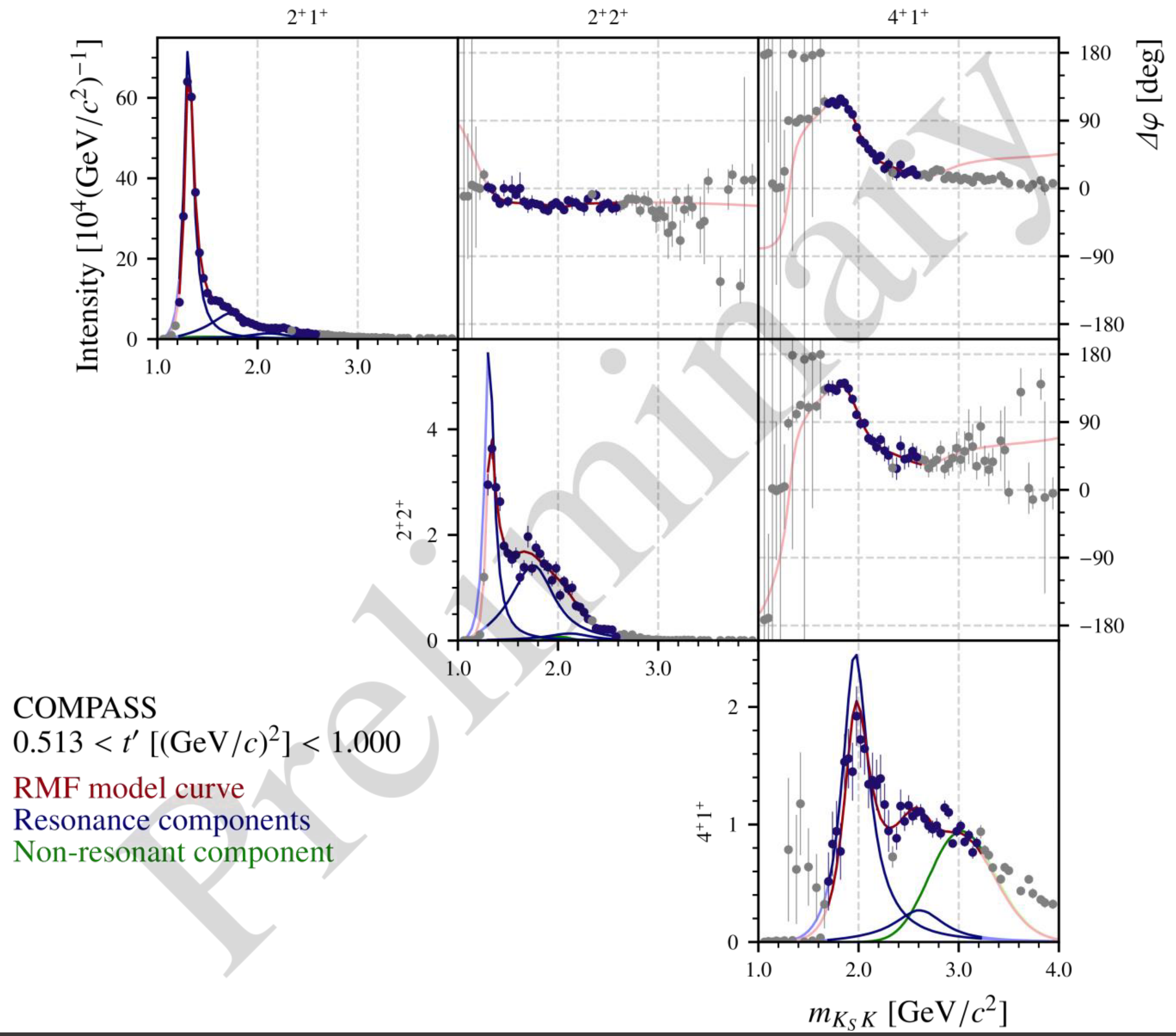

The $J^{PC} = 4^{++}$ Sector in $K_S^0 K^-$

$a_4(1970)$:

- Precise measurement of the well-known state
- Clear peak and phase movement well-described

$$m_0 = 1952.2 \pm 1.8\,^{+3.0}_{-3.5}$$
$$\Gamma_0 = 327 \pm 4\,^{+6}_{-6}$$

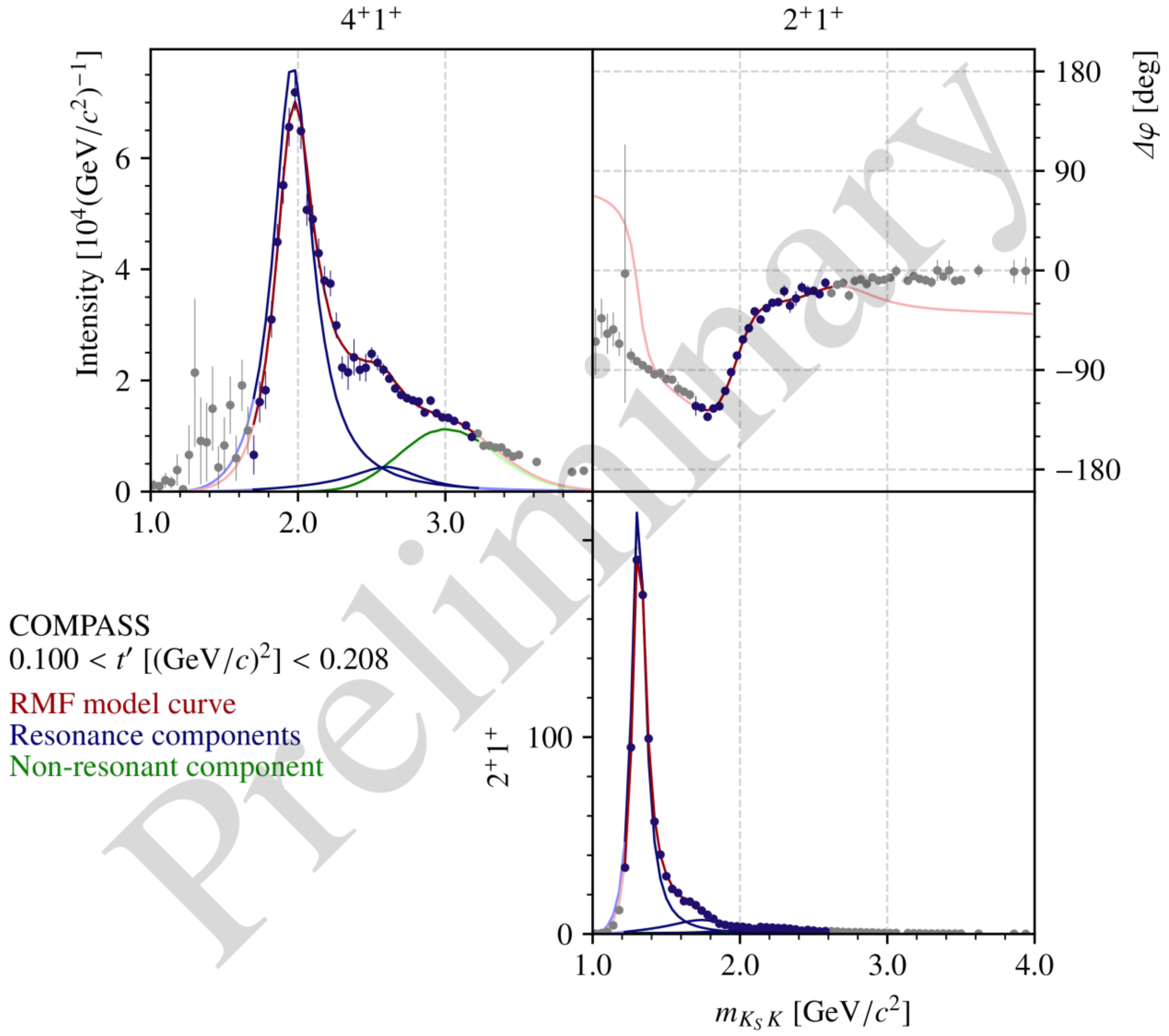

The $J^{PC} = 4^{++}$ Sector in $K_S^0 K^-$

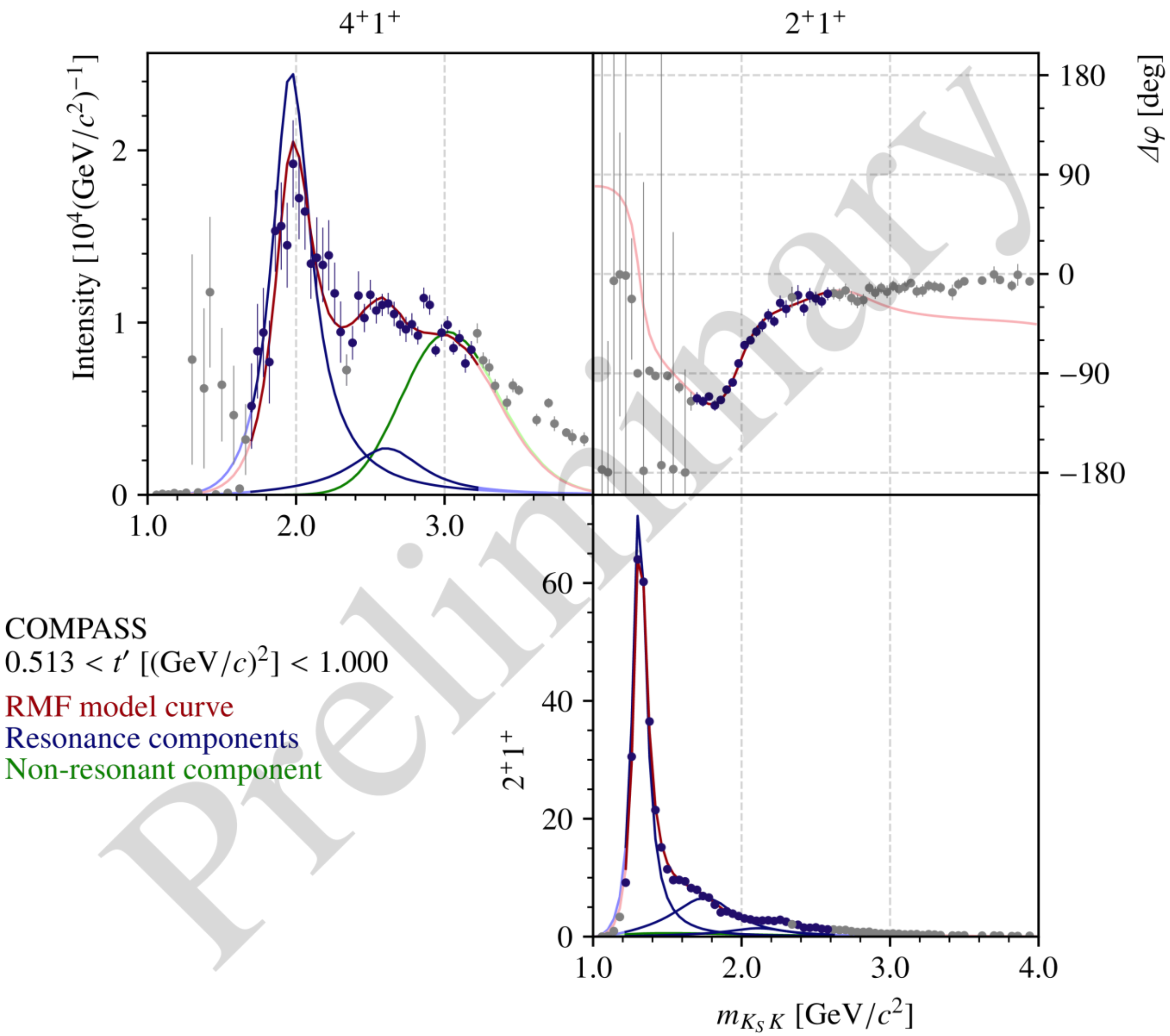

The $J^{PC} = 6^{++}$ Sector in $K_S^0 K^-$

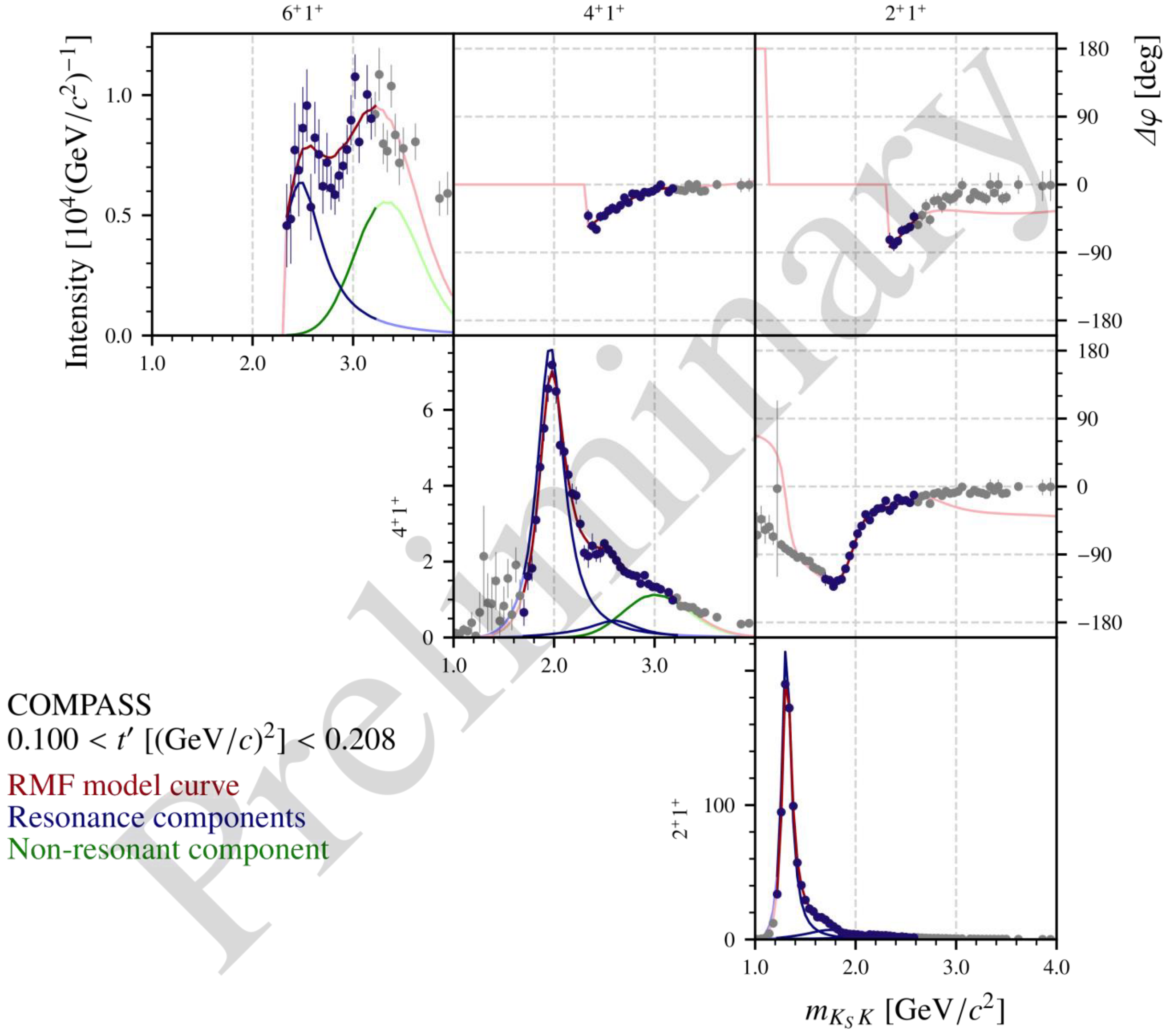

The $J^{PC} = 6^{++}$ Sector in $K_S^0 K^-$

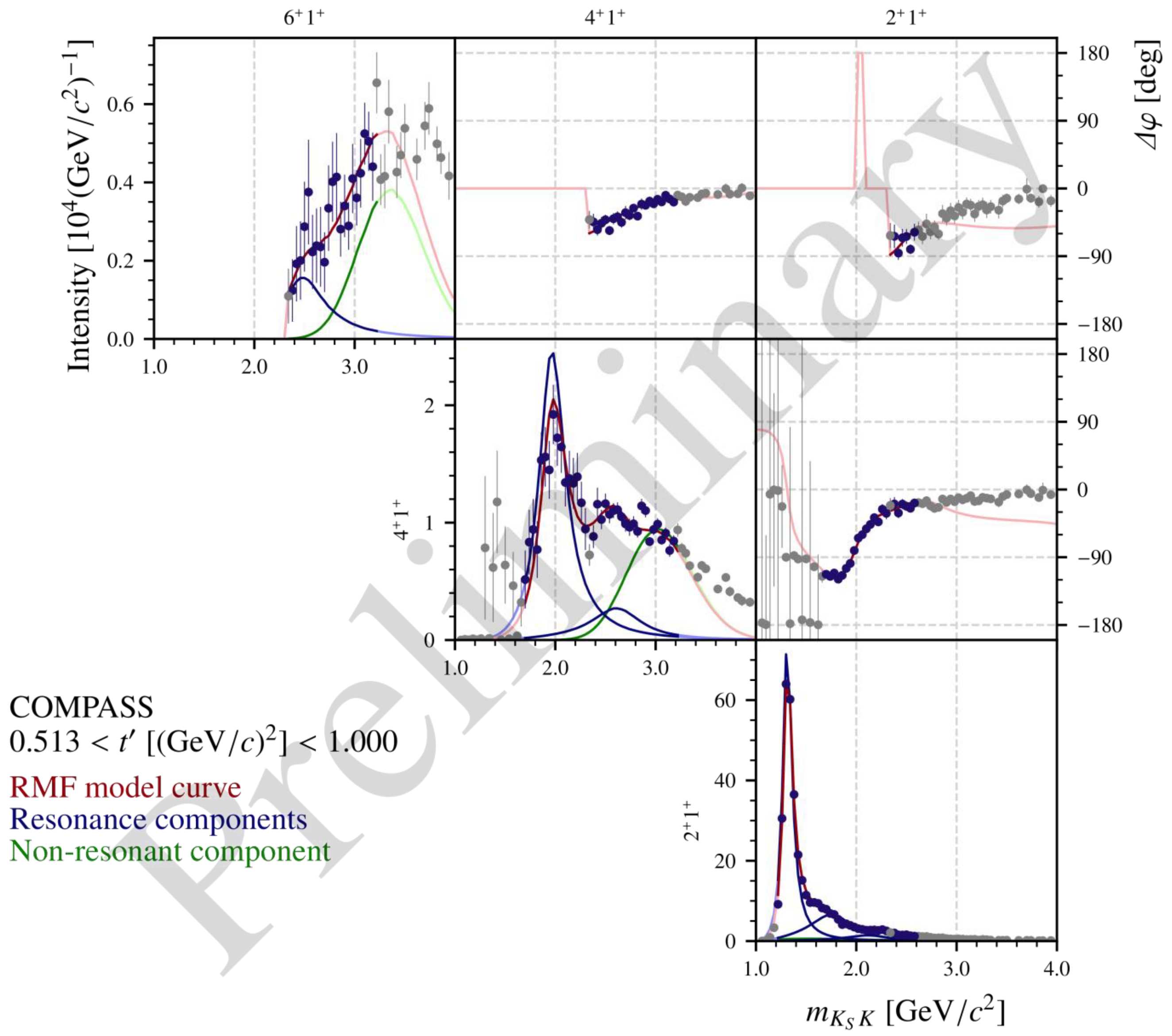

$\omega(782)$ Selection

- Reconstruction of $\omega(782)$ from $\pi^-\pi^0\pi^+$ decay

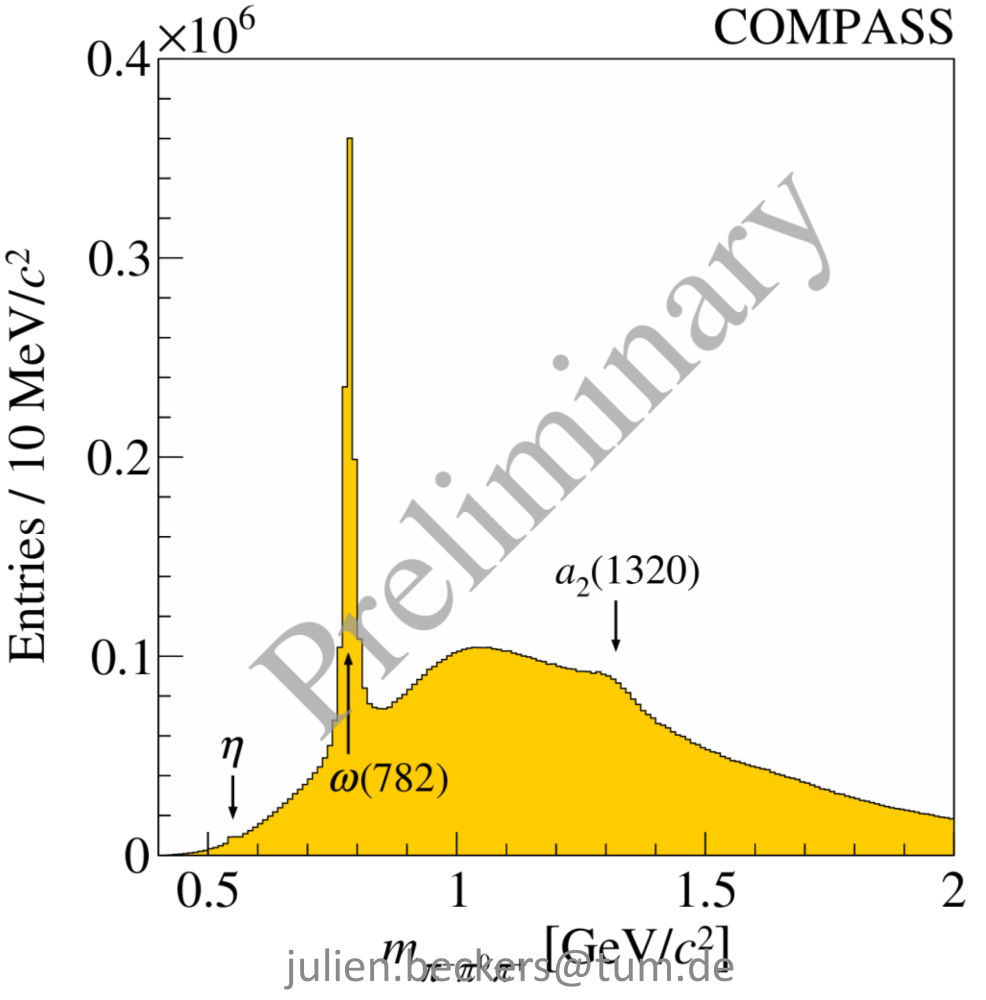

$\omega(782)$ Selection

- Reconstruction of $\omega(782)$ from $\pi^-\pi^0\pi^+$ decay
- Select events with exactly one $\pi^-\pi^0\pi^+$ combination within $\pm\,3\sigma_\omega$ around the fitted m_ω

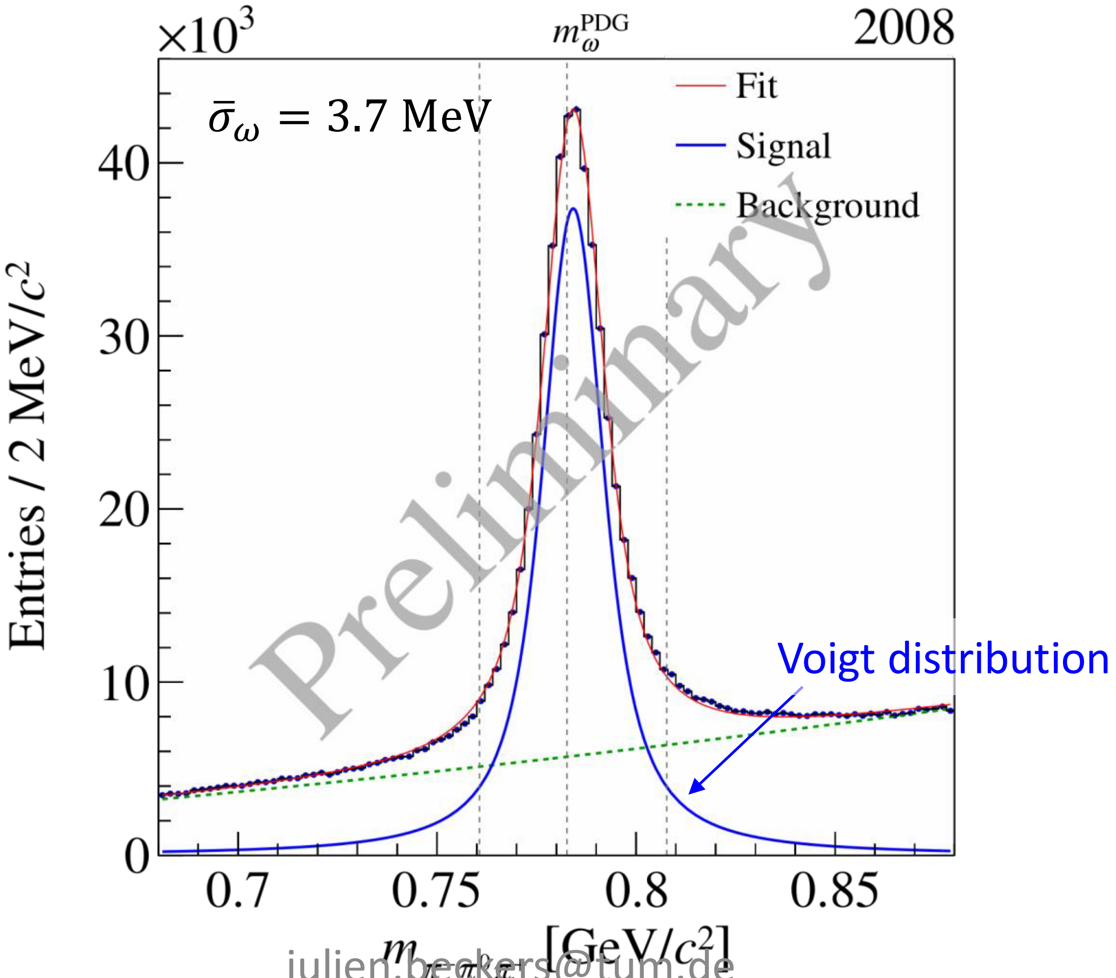

Wave Selection

- Method used for 5π and $K\pi\pi$
- Modified log-likelihood with penalties:
  - Cauchy regularization to suppress small waves
  - Connected bins over m_X to smoothen $\mathcal{T}_i(m_X)$
- Wave pool:
  - $J \leq 7, M \leq 2, \epsilon = +$
  - $\xi \to \pi\pi$: $\rho(770), \rho_3(1690)$
  - $\xi \to \omega\pi$: $b_1(1235), \rho(1450), \rho_3(1690)$
  - $L \leq 7, S \leq 2$ except for $\rho_3(1690) \to \omega\pi$ $(S = 3)$
  - 434 waves + flat wave

Notation:

$i = J^P M^\epsilon\ [\xi l]\ b\ LS$

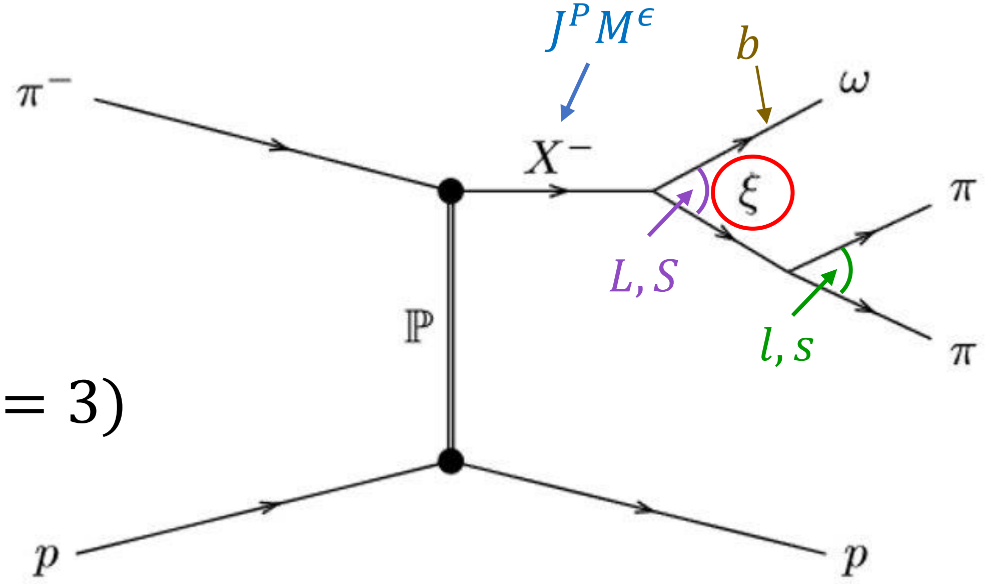

Extracted Resonance Parameters in $\omega\pi^-\pi^0$

Resonance	m_0 [MeV/c^2]	Γ_0 [MeV/c^2]
$\pi(1800)$	$1768 \pm 6^{+21}_{-16}$	$320 \pm 9^{+14}_{-16}$
$a_1(1640)$	$1660 \pm 20^{+30}_{-50}$	$370 \pm 30^{+20}_{-50}$
$a_1(1930)$	$1970 \pm 20^{+30}_{-40}$	$230 \pm 30^{+140}_{-40}$
$\pi_1(1600)$	$1723 \pm 6^{+37}_{-14}$	$336 \pm 10^{+96}_{-33}$
$\pi_2(1670)$	$1698 \pm 6^{+18}_{-7}$	$296 \pm 11^{+30}_{-15}$
$\pi_2(1880)$	$1876 \pm 4^{+4}_{-4}$	$166 \pm 8^{+8}_{-18}$
π_2''	$2142 \pm 12^{+15}_{-21}$	$304 \pm 21^{+14}_{-34}$
a_3	$2080 \pm 10^{+40}_{-40}$	$560 \pm 20^{+100}_{-100}$
$a_4(1970)$	$1973 \pm 3^{+15}_{-8}$	$311 \pm 8^{+10}_{-46}$
$\pi_4(2250)$	$2198 \pm 12^{+25}_{-27}$	$550 \pm 30^{+90}_{-40}$
$a_6(2450)$	$2558 \pm 31^{+12}_{-73}$	$600 \pm 90^{+60}_{-170}$

The $J^{PC} = 0^{-+}$ in $\omega\pi^-\pi^0$

- Clear peak and rising phase at $1.8\ \mathrm{GeV}/c^2$ in $0^-0^+[\rho P]\omega\ P1$

$\Rightarrow \pi(1800)$

- $m_0 = 1768 \pm 6^{+21}_{-16}$
- $\Gamma_0 = 320 \pm 9^{+14}_{-16}$

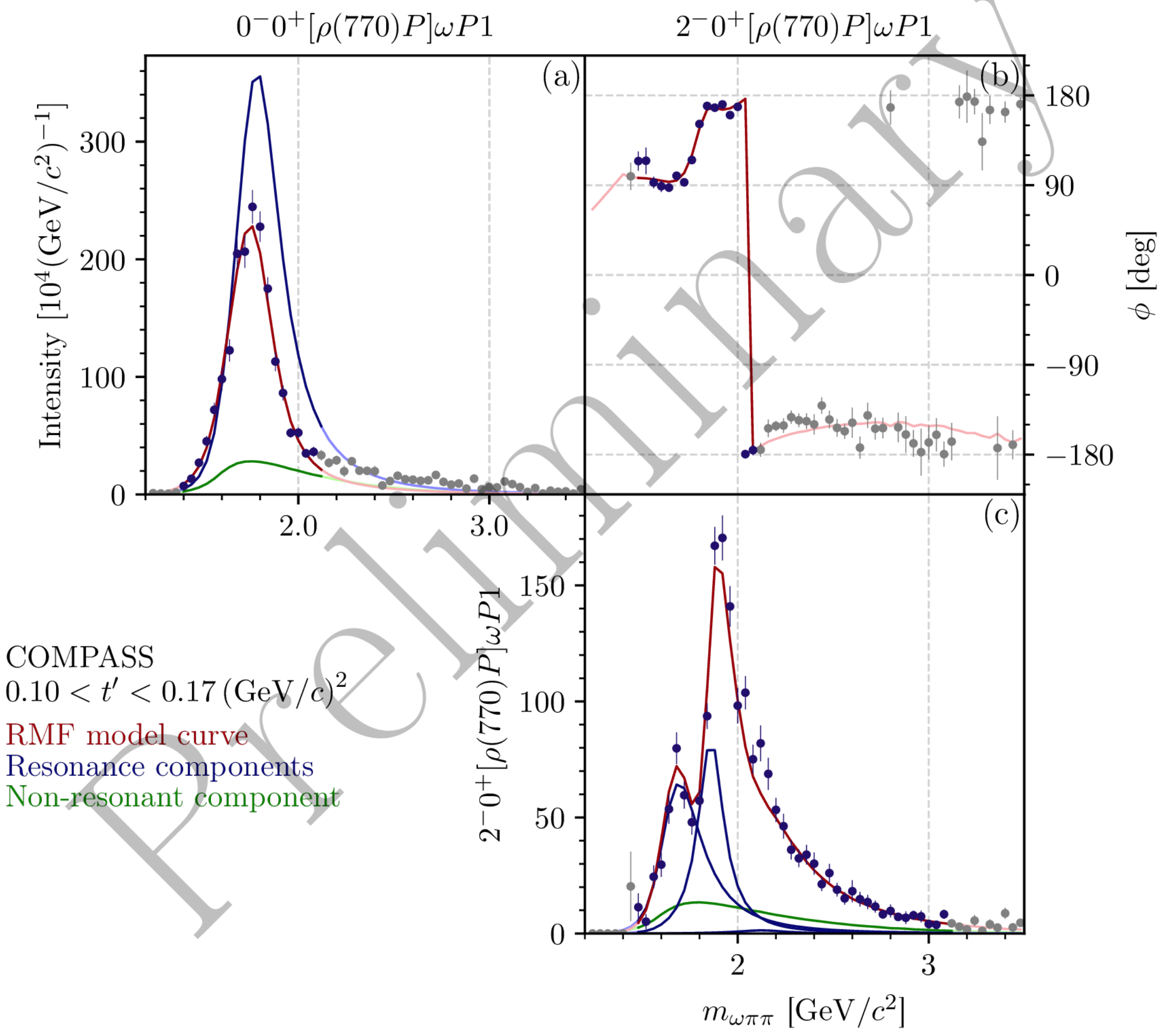

The $J^{PC} = 1^{++}$ in $\omega\pi^-\pi^0$

- Threshold effects at $1.5\ \mathrm{GeV}/c^2$
- Phase motion between two $\rho(770)\omega$ waves
  - $\Rightarrow$ Indication for multiple a_1 resonances

	m_0	Γ_0
$a_1(1640)$	$1660 \pm 20^{+30}_{-50}$	$370 \pm 30^{+20}_{-50}$
$a_1(1930)$	$1970 \pm 20^{+30}_{-40}$	$230 \pm 30^{+140}_{-40}$

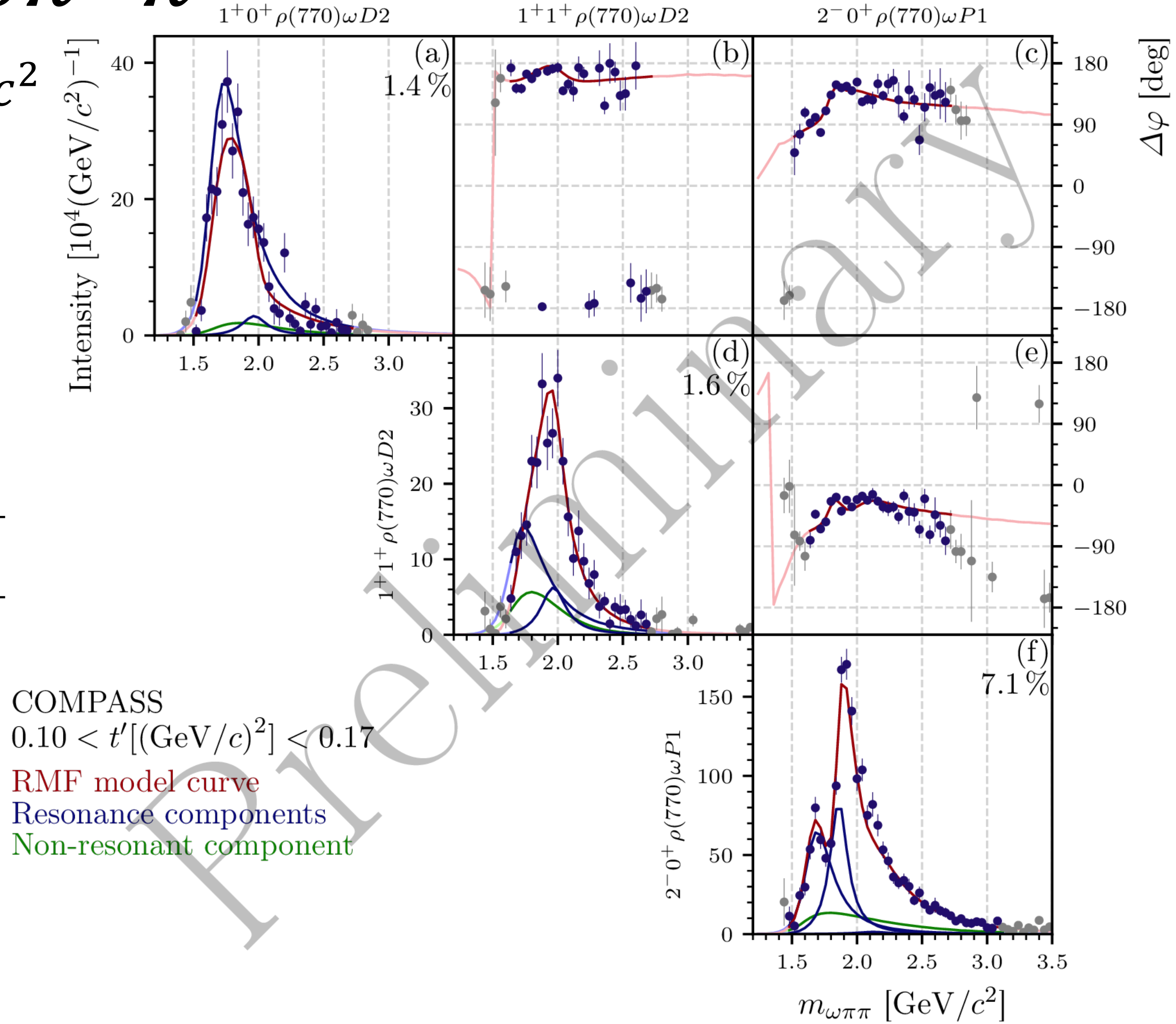

The $J^{PC} = 1^{-+}$ in $\omega\pi^-\pi^0$

- Clear Breit-Wigner signals in $b_1\pi$ and $\rho\omega$ waves around $1.7\ \mathrm{GeV}/c^2$

  $\Rightarrow \pi_1(1600)$:
  - $m_0 = 1723 \pm 6^{+37}_{-14}$
  - $\Gamma_0 = 336 \pm 10^{+96}_{-33}$
- Only b_1 D-wave in this RMF
- Close to no background in all waves
- No indication for excited $\pi_1(2015)$ seen by BNL E852 in $b_1\pi$ waves

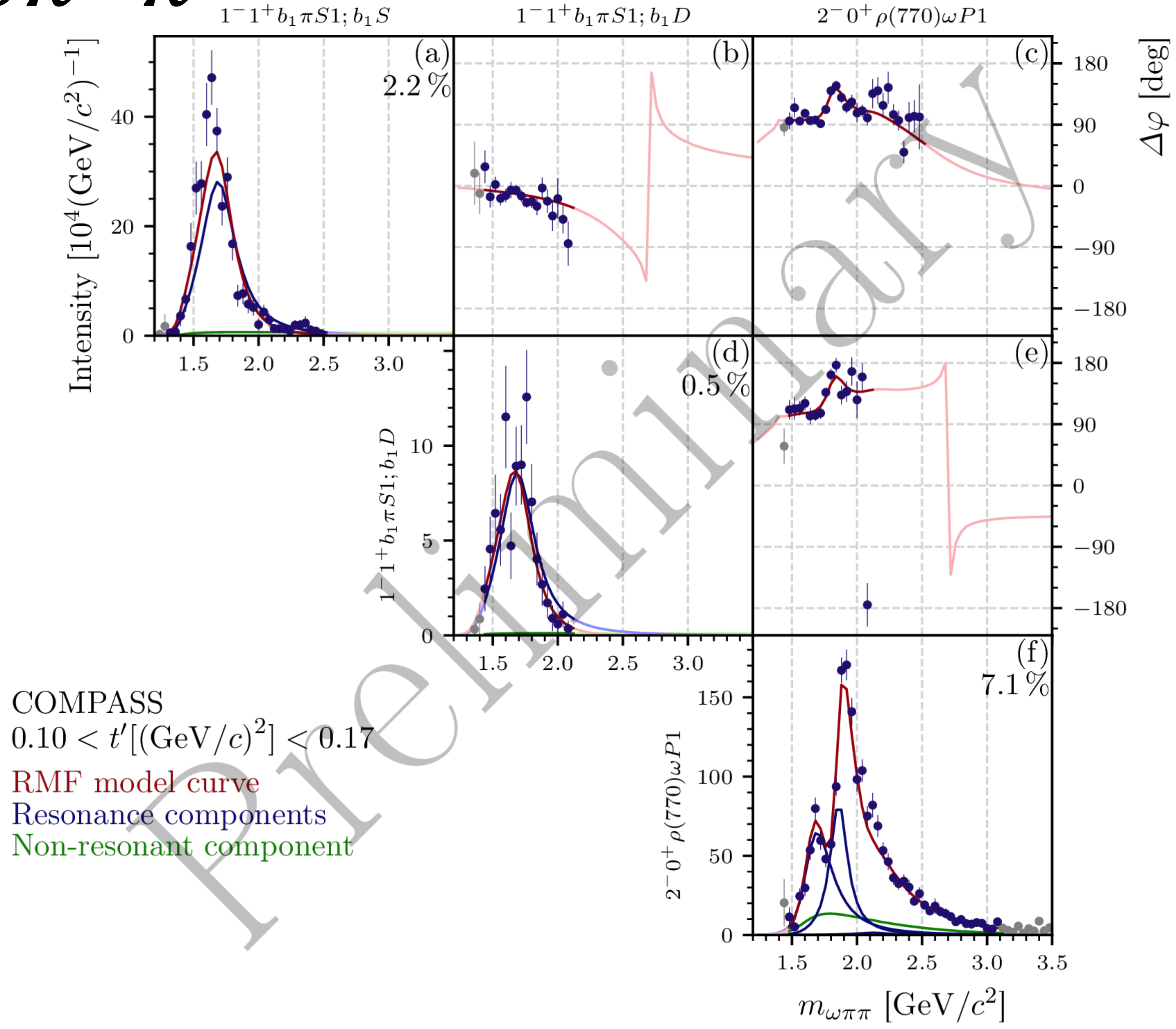

The $J^{PC} = 2^{++}$ in $\omega\pi^-\pi^0$

- Most dominant sector due to $a_2(1320)$
  - $a_2(1320)$ dominates all partial waves
- Thresholds around $1.5\ \mathrm{GeV}/c^2$ due to shrinking phase-space volume at low masses
  - Strong leakage between 2^{++} waves
- Discontinuity at threshold and strong phase-space effects complicate fitting of a_2 states

$\Rightarrow$ Current models fail

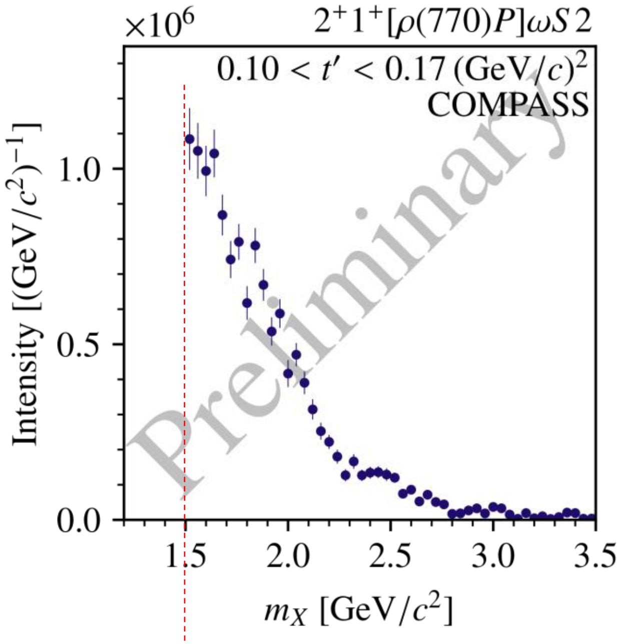

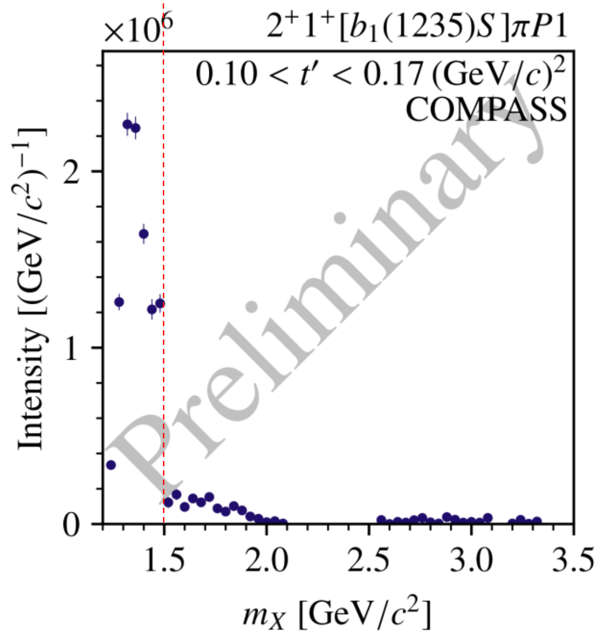

The $J^{PC} = 2^{-+}$ in $\omega\pi^-\pi^0$

- Fit includes 4 waves
- Complex phase motion between waves
- Sufficient description of all four waves requires three resonances
- Destructive interference only significant in $2^-0^+\rho(770)\omega\ P2$

	m_0	Γ_0
$\pi_2(1670)$	$1698 \pm 6^{+18}_{-7}$	$296 \pm 11^{+30}_{-15}$
$\pi_2(1880)$	$1876 \pm 4^{+4}_{-4}$	$166 \pm 8^{+8}_{-18}$
π_2''	$2142 \pm 12^{+15}_{-21}$	$304 \pm 21^{+14}_{-34}$

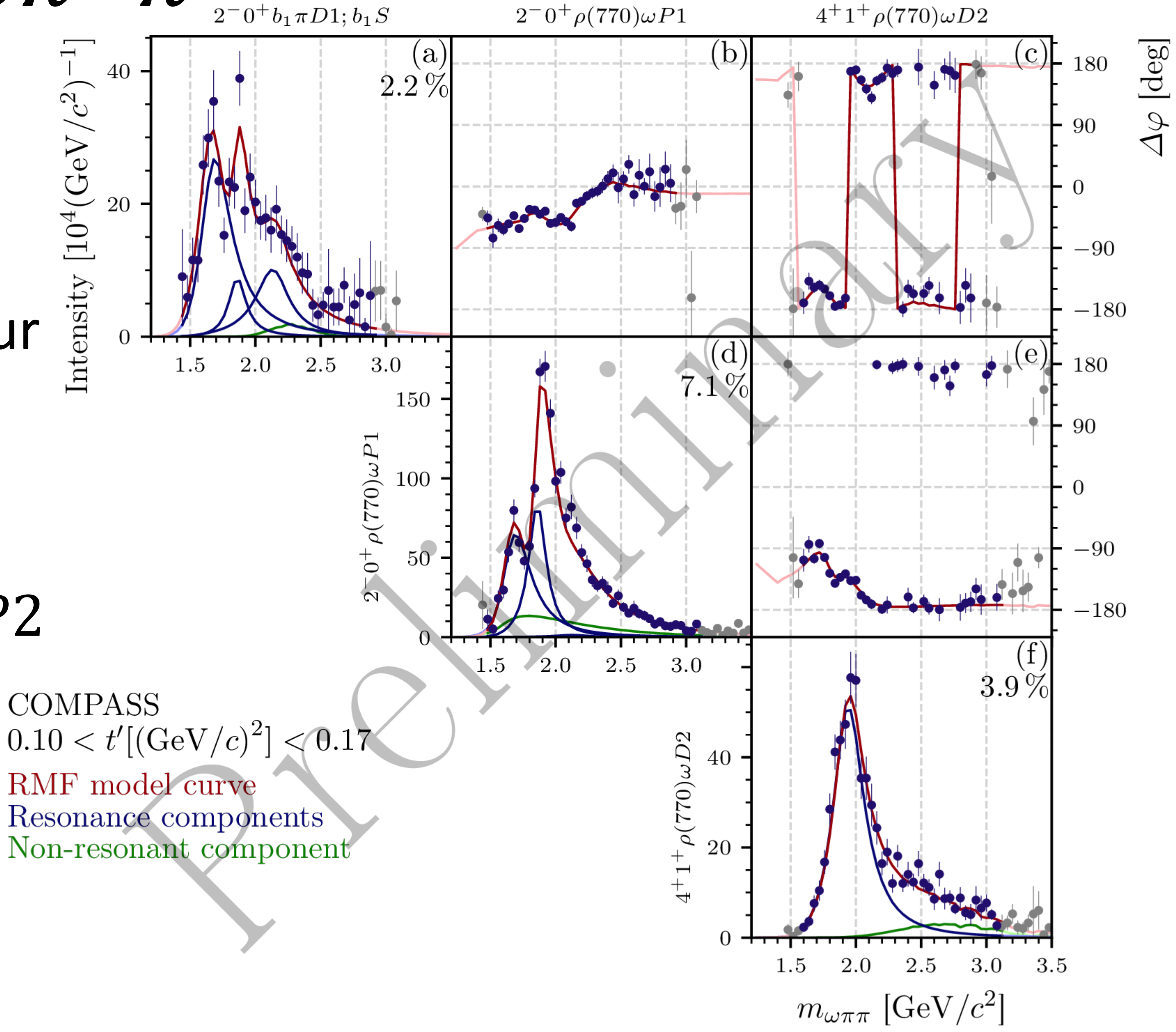

The $J^{PC} = 2^{-+}$ in $\omega\pi^-\pi^0$

- Fit includes 4 waves
- Complex phase motion between waves
- Sufficient description of all four waves requires three resonances
- Destructive interference only significant in $2^-0^+\rho(770)\omega\ P2$

	m_0	Γ_0
$\pi_2(1670)$	$1698 \pm 6^{+18}_{-7}$	$296 \pm 11^{+30}_{-15}$
$\pi_2(1880)$	$1876 \pm 4^{+4}_{-4}$	$166 \pm 8^{+8}_{-18}$
π_2''	$2142 \pm 12^{+15}_{-21}$	$304 \pm 21^{+14}_{-34}$

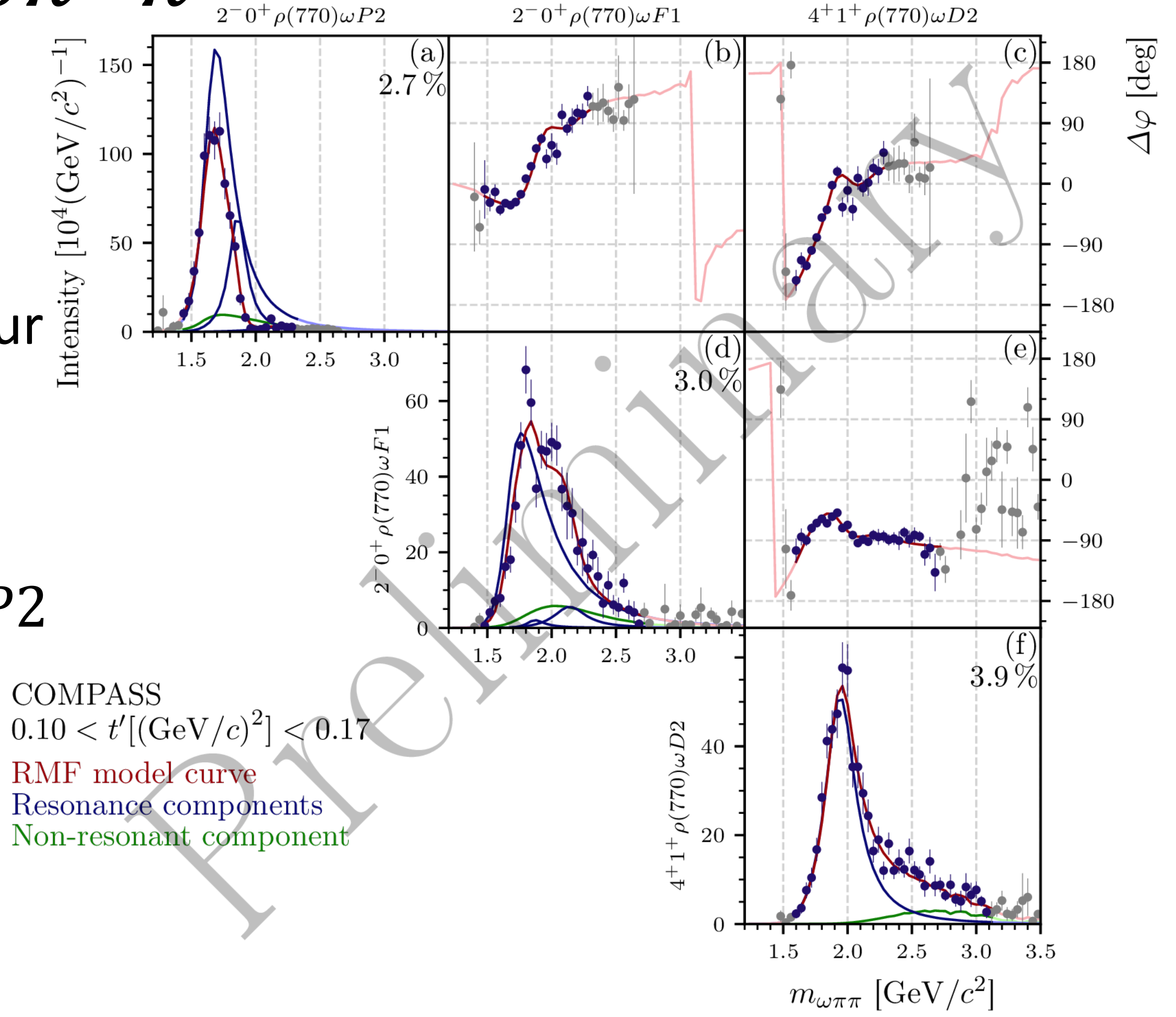

julien.beckers@tum.de

The $J^{PC} = 3^{++}$ in $\omega\pi^-\pi^0$

- Clear resonance-like signals in $b_1\pi$, $\rho_3\pi$, and 2 $\rho\omega$ waves around 2.0 GeV/c^2
- Phases and intensities are well described by single BW
  - => No indication for additional resonances

$\Rightarrow a_3$:

- $m_0 = 2080 \pm 10^{+40}_{-40}$
- $\Gamma_0 = 560 \pm 20^{+100}_{-100}$

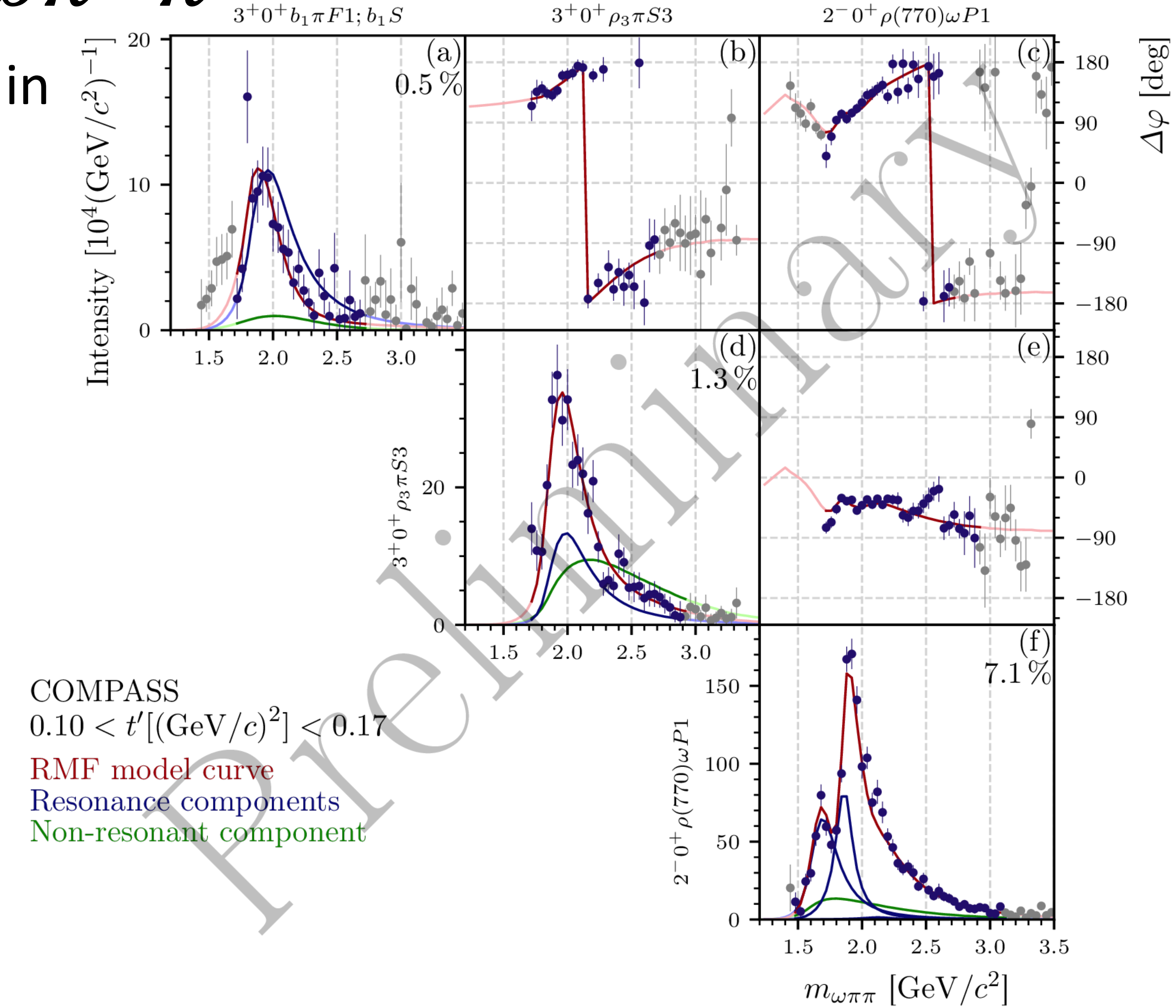

julien.beckers@tum.de

The $J^{PC} = 3^{++}$ in $\omega\pi^-\pi^0$

- Clear resonance-like signals in $b_1\pi$, $\rho_3\pi$, and 2 $\rho\omega$ waves around 2.0 GeV/c^2
- Phases and intensities are well described by single BW
  - => No indication for additional resonances

$\Rightarrow a_3$:
- $m_0 = 2080 \pm 10^{+40}_{-40}$
- $\Gamma_0 = 560 \pm 20^{+100}_{-100}$

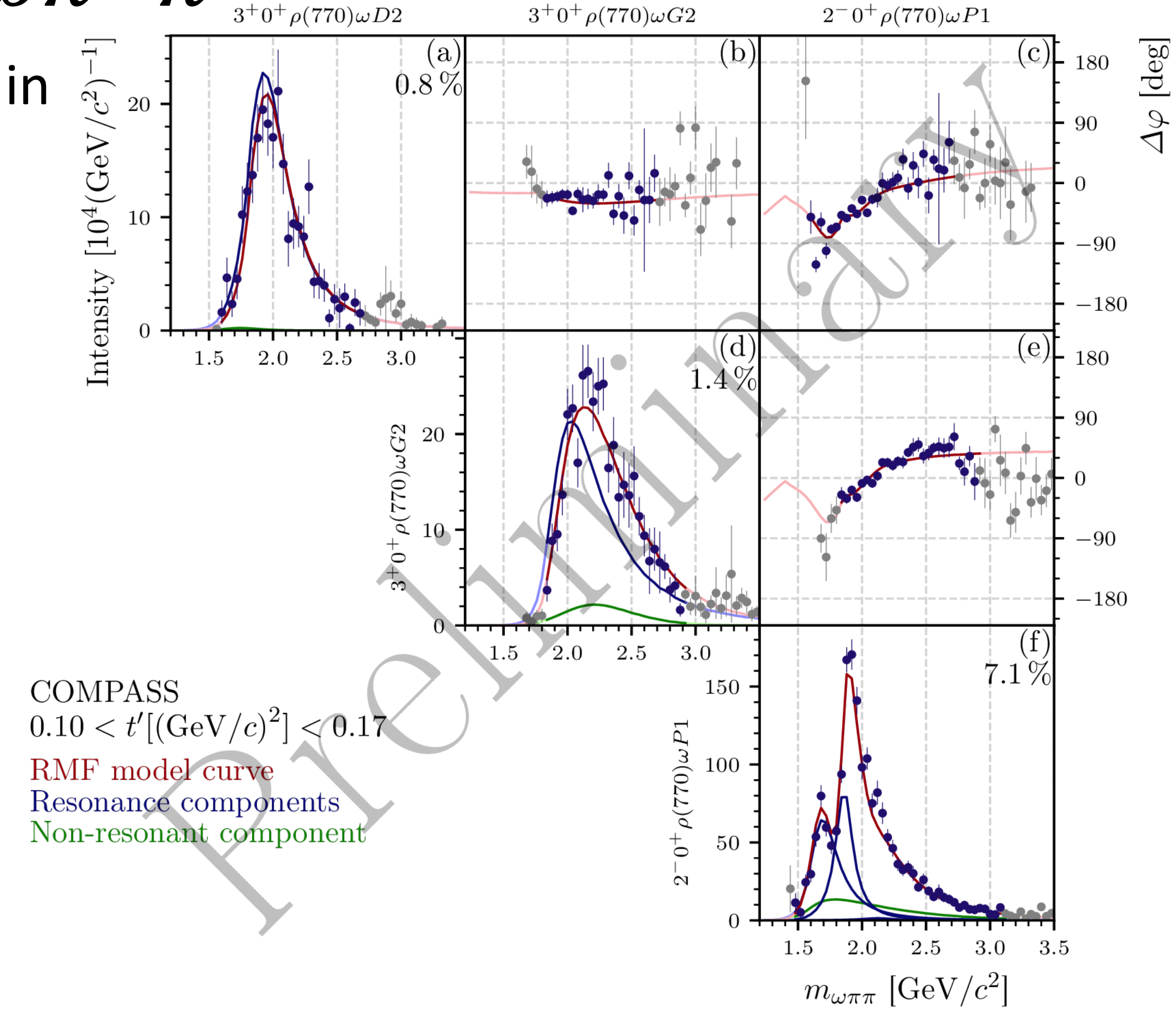

julien.beckers@tum.de

The $J^{PC} = 4^{++}$ in $\omega\pi^-\pi^0$

- Dominant peak and rising phase around 2.0 GeV/c^2 in both $b_1\pi$ and $\rho\omega$ waves

$\Rightarrow a_4(1970)$:

- $m_0 = 2558 \pm 31^{+12}_{-73}$
- $\Gamma_0 = 600 \pm 90^{+60}_{-170}$

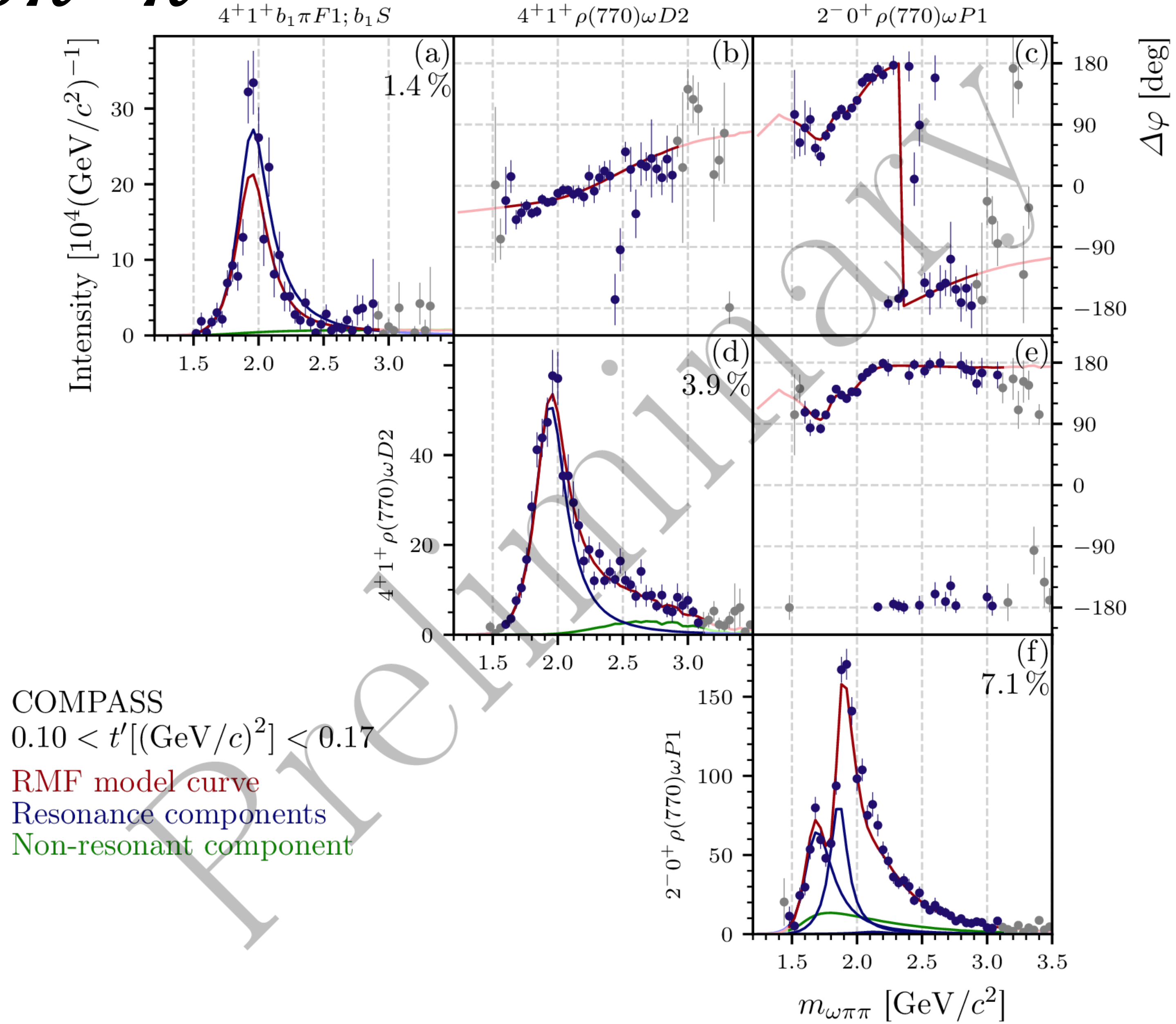

The $J^{PC} = 4^{-+}$ in $\omega\pi^-\pi^0$

- Peaks in the intensities of $b_1\pi$, $\rho_3\pi$, and $\rho\omega$ waves around 2.3 GeV/c^2

$\Rightarrow \pi_4(2250)$:

  - $m_0 = 2198 \pm 12^{+25}_{-27}$
  - $\Gamma_0 = 550 \pm 30^{+90}_{-40}$

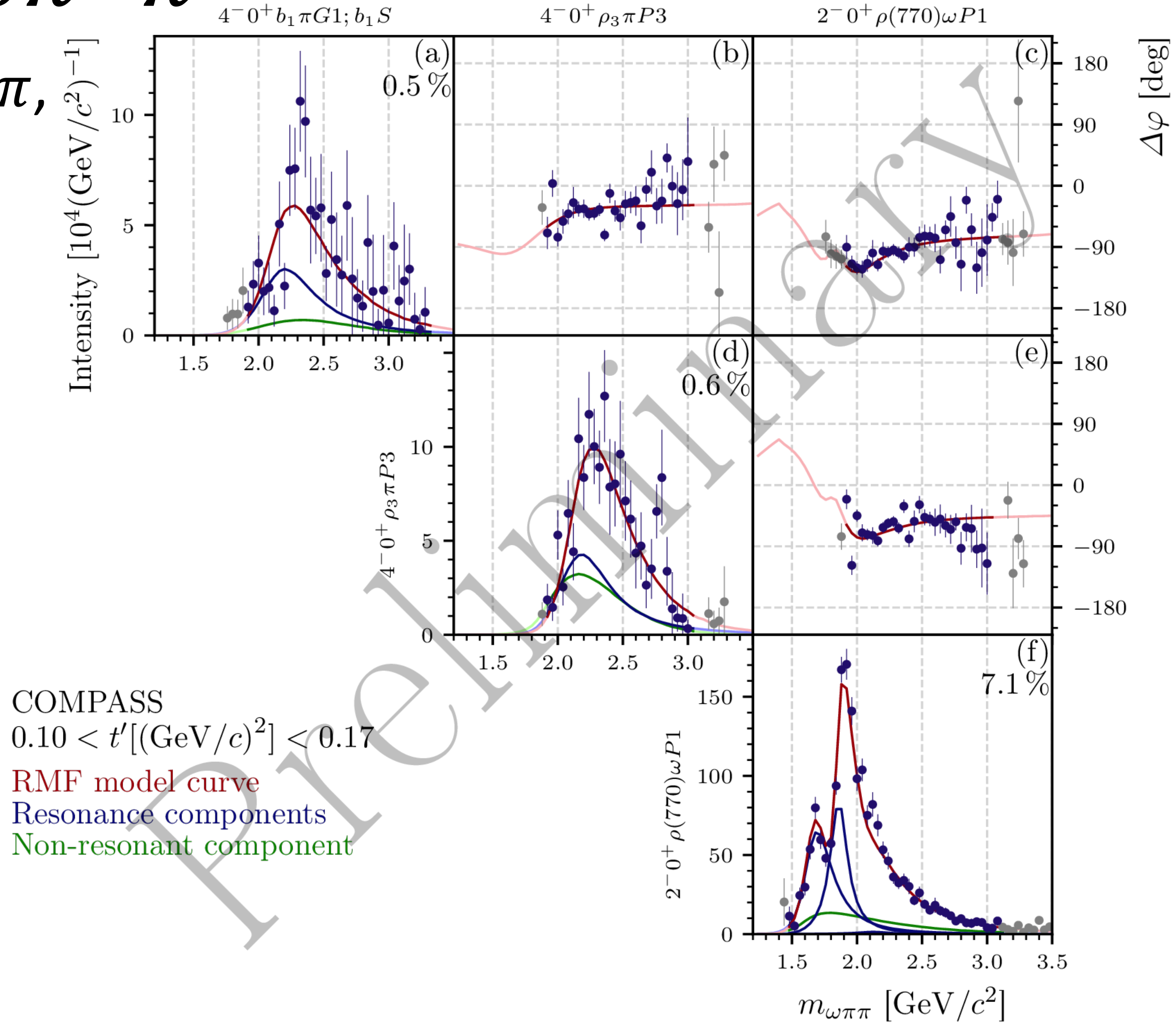

The $J^{PC} = 4^{-+}$ in $\omega\pi^-\pi^0$

- Peaks in the intensities of $b_1\pi$, $\rho_3\pi$, and $\rho\omega$ waves around $2.3\ \mathrm{GeV}/c^2$

$\Rightarrow \pi_4(2250)$:

- $m_0 = 2198 \pm 12^{+25}_{-27}$
- $\Gamma_0 = 550 \pm 30^{+90}_{-40}$

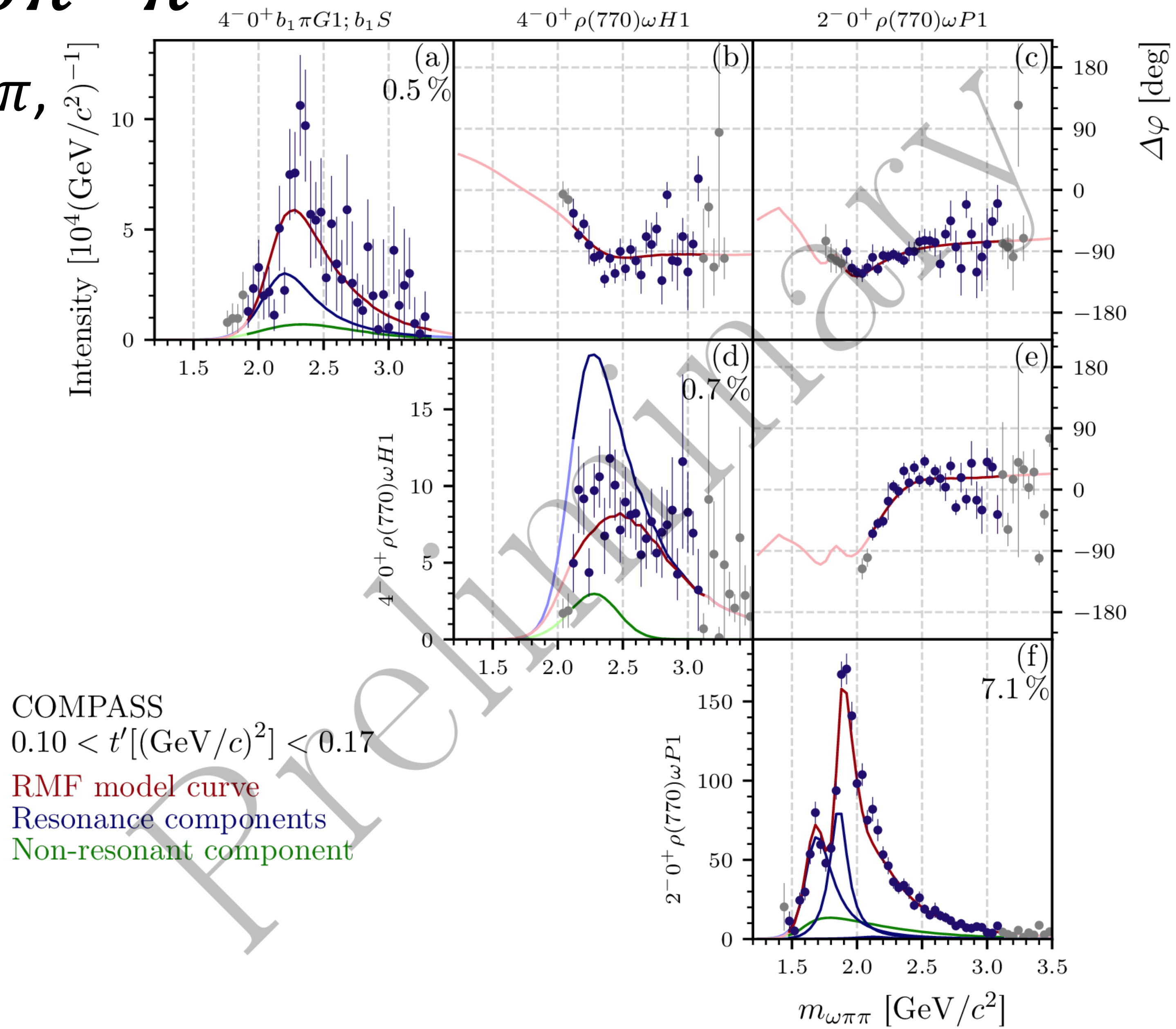

The $J^{PC} = 6^{++}$ in $\omega\pi^-\pi^0$

- Peaks in the intensities of $b_1\pi$, $\rho_3\pi$, and $\rho\omega$ waves around 2.5 GeV/c^2
- Rising phase for these waves w.r.t. $2^-0^+[\rho P]\omega\ P1$

$\Rightarrow a_6(2450)$:
  - $m_0 = 2558 \pm 31^{+12}_{-73}$
  - $\Gamma_0 = 600 \pm 90^{+60}_{-170}$

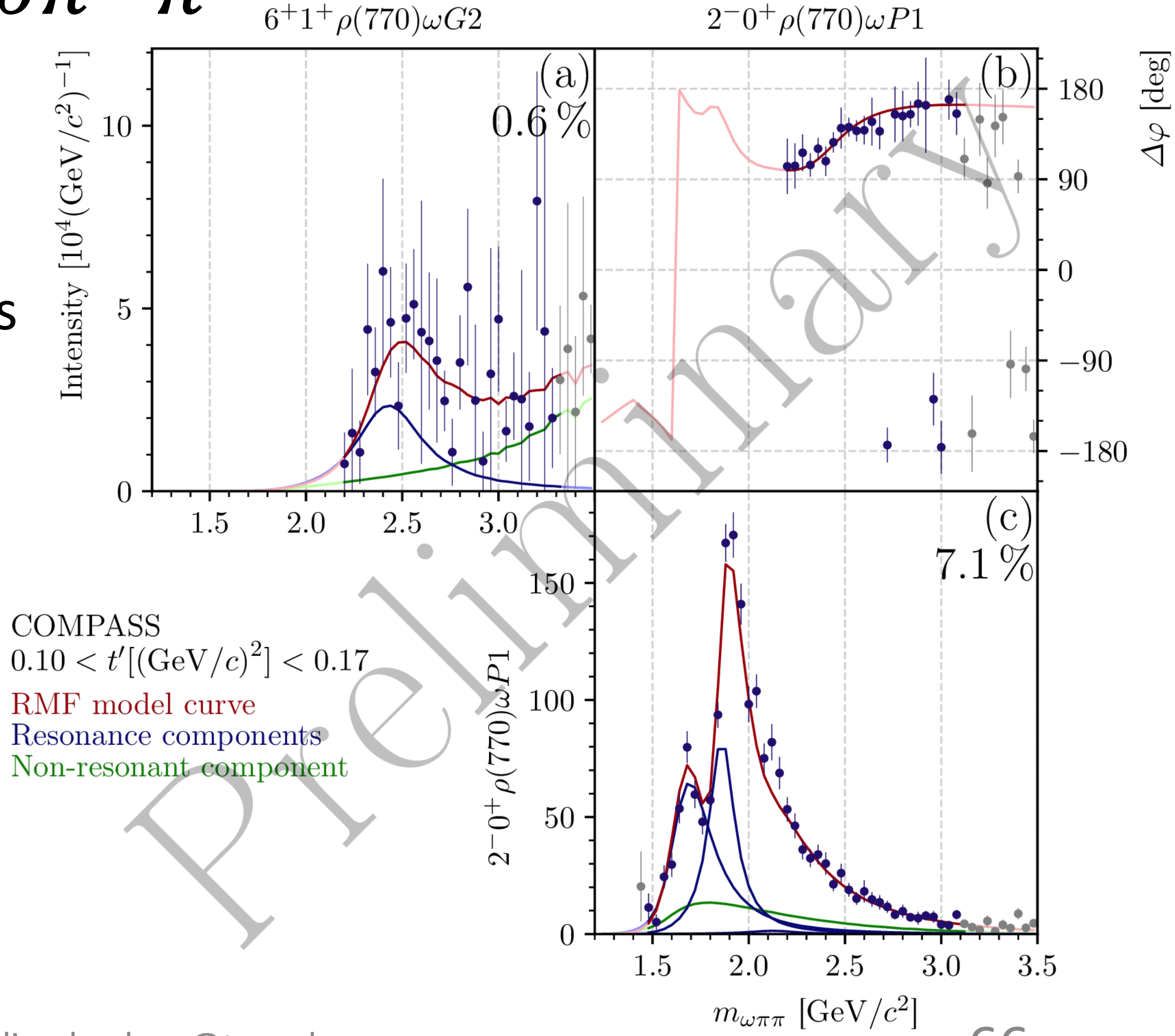

The $J^{PC} = 6^{++}$ in $\omega\pi^-\pi^0$

- Peaks in the intensities of $b_1\pi$, $\rho_3\pi$, and $\rho\omega$ waves around 2.5 GeV/c^2
- Rising phase for these waves w.r.t. $2^-0^+[\rho P]\omega\ P1$

$\Rightarrow a_6(2450)$:

- $m_0 = 2558 \pm 31^{+12}_{-73}$
- $\Gamma_0 = 600 \pm 90^{+60}_{-170}$